

# Quantum Annealing and Analog Quantum Computation

Arnab Das\* and Bikas K. Chakrabarti†

*Theoretical Condensed Matter Physics Division and  
Centre for Applied Mathematics and Computational Science, Saha Institute of Nuclear Physics, 1/AF,  
Bidhannagar, Kolkata-700064, India.*

We review here the recent success in quantum annealing, i.e., optimization of the cost or energy functions of complex systems utilizing quantum fluctuations. The concept is introduced in successive steps through the studies of mapping of such computationally hard problems to the classical spin glass problems. The quantum spin glass problems arise with the introduction of quantum fluctuations, and the annealing behavior of the systems as these fluctuations are reduced slowly to zero. This provides a general framework for realizing analog quantum computation.

PACS numbers: 0.2.10.Ox, 0.2.60.Pn, 0.2.70.Ss, 0.3.65.Xp, 03.67.Lx, 64.60.Cn, 64.70.Pf

## Contents

<b>I. Introduction</b>	1
<b>II. Optimization and Annealing</b>	3
A. Combinatorial Optimization Problems	3
B. Statistical Mechanics of the Optimization Problems and Thermal Annealing	4
C. Spin Glass and Optimization	5
1. Finding The Ground States of the Classical Spin Glasses	5
2. The Traveling Salesman Problem	6
D. Quantum Spin Glasses and Annealing	7
<b>III. Quantum Annealing</b>	9
A. Quantum Monte Carlo Annealing	10
1. A Short-Range Spin Glass	11
2. The Traveling Salesman Problem	12
3. Random Field Ising Model: How a Choice of Kinetic Term Improves Annealing Results	13
B. Quantum Annealing Using Real-time Adiabatic Evolution	13
C. Annealing of a Kinetically Constrained System	16
D. Experimental Realization of Quantum Annealing	17
<b>IV. Convergence of Quantum Annealing Algorithms</b>	18
<b>V. Quantum Quenching</b>	18
<b>VI. Summary and Discussions</b>	18
<b>Acknowledgments</b>	19
<b>VII. Appendix</b>	19
1. Suzuki-Trotter Formalism	19
2. Quantum Quenching of a Long Range TIM	20
<b>References</b>	20

## I. INTRODUCTION

Utilization of quantum mechanical tunneling through classically localized states in annealing of glasses has opened up a new paradigm for solving hard optimization problems through adiabatic reduction of quantum fluctuations. This will be introduced and reviewed here.

Consider the example of a ferromagnet consisting of  $N$  tiny interacting magnetic elements; the spins. For a macroscopic sample  $N$  is very large; of the order of Avogadro number. Assume that each spin can be in any of the two simple states: up or down. Also, the pairwise interactions between the spins are such that the energy of interaction (potential energy or PE) between any pair of spins is negative (smaller) if both the spins in the pair are in the same state and is positive (higher) if their states differ. As such, the collective energy of the  $N$ -spin system (given by the Hamiltonian  $\mathcal{H}$ ) is minimum when all the spins are aligned in the same direction; all up or all down, giving the full order. We call these two minimum energy configurations the ground states. The rest of the  $2^N$  configurations are called excited states. The plot of the interaction energy of the whole system with respect to the configurations is called the potential energy-configuration landscape, or simply, the potential energy landscape (PEL). For a ferromagnet, this landscape has a smooth double-valley structure (two mirror-symmetric valleys with the two degenerate ground states, all up and all down, at their respective bottoms). At zero-temperature the equilibrium state is the state of minimum potential energy, and the system stably resides at the bottom of any of the two valleys. At finite temperature, the thermal fluctuations allow the system to visit higher energy configurations with some finite probability (given by the Boltzmann factor) and thus the system spends time in other part of the PEL also. The proba-

\*Electronic address: [arnab.das@saha.ac.in](mailto:arnab.das@saha.ac.in)

†Electronic address: [bikask.chakrabarti@saha.ac.in](mailto:bikask.chakrabarti@saha.ac.in)

bility that a system is found in a particular macroscopic state depends not only on the energy of the state (as at zero temperature), but also on its entropy. The thermodynamic equilibrium state corresponds to the minimum of a thermodynamic potential called free energy  $F$  given by the difference between the energy of the state and the product of its entropy and the temperature. At zero-temperature, the minima of the free energy coincides with the minimum for energy and one gets the highest order (magnetization). As the temperature is increased, the contribution of entropy gets magnified and the minimum of the free energy is shifted more and more towards the states with lower and lower order or magnetization, until at (and beyond) some transition temperature  $T_c$ , the order disappears completely. For antiferromagnetic systems, the spin-spin pair interactions are such that it is lower if the spins in the pair are in opposite states, and higher if their states are same. For antiferromagnets one can still define a sub-lattice order or magnetization and the PEL still has the double-well structure like in a ferromagnet for short range interactions. The free energy and the order-disorder transition also shows identical behavior as observed for a ferromagnet.

In spin glasses, where different spin-spin interactions are randomly ferromagnetic or antiferromagnetic and frozen in time (quenched disorder), the PEL becomes extremely rugged; various local and global minima trapped between potential energy barriers appears in the PEL. The ruggedness and the degeneracies in the minima comes from the effect of frustration or competing interactions between the spins; none of the spin states on a cluster or a placket is able to satisfy all the interactions in the cluster. The locally optimal state for the spins in the cluster is therefore degenerate and frustrated.

Similar situations occur for multivariate optimization problems like the traveling salesman problem (TSP). Here a salesman has to visit  $N$  cities placed randomly on a plane (country). Of the  $N!/N$  distinct tours passing through each city once, only few corresponds to the minimum (ground state) travel distance or travel cost. The rests corresponds to the higher costs (excited states). The cost function, when plotted against different tour configurations, gives a similar rugged landscape, equivalent to the PEL of a spin glass (henceforth we will use PEL to mean cost-configuration landscapes also).

Obviously, an exhaustive search for the global minimum of a rugged PEL requires an exponentially large (or higher) number (in  $N$ ) of searches ( $2^N$  or  $N!$  order of searches for an  $N$ -spin spin glass and an  $N$ -city TSP respectively). The computational effort or time for such searches are therefore generally not bounded by any polynomial in the problem size  $N$ . Alternatively, a gradual energy or cost dissipative dynamics (annealing), with Boltzmann like thermal fluctuations or some noise factor (in order to get out of the the local minima) in the PEL may help reaching deep enough minima more easily. This simulated thermal annealing scheme is considered to be a very successful technique now. However,

such a technique often fails if the barrier heights between the minima diverges (or become very high), as in case of a spin glass, due to frequent trapping of the system in such local minima (glassy behavior). In case such barriers are very narrow, quantum-mechanical fluctuations (fluctuations in a quantum observable due to its non-commutativity with the Hamiltonian of the system) can help tunneling through them, thereby leading to successful quantum annealing (see. Fig. 1).

We introduce here these ideas in details through successive steps.

a) The physics of classical spin glasses has already contributed enormously to our knowledge of the landscape structure of the energy or the thermodynamic potentials and that of the unusually slow (glassy) dynamics of many-body systems in the presence of frustration and disorder. Mapping of computationally hard problems, like the traveling salesman problem etc, to classical spin glass models also helped understanding their complexity.

b) The ground (and some low-lying) state structures of frustrated random systems in the presence of quantum fluctuations have also been studied in the context of quantum spin glasses. It has been shown that because of the possibility of tunneling through the barriers in the potential energy landscape, quantum fluctuations can help the dynamics to be ‘more ergodic’ than the dynamics induced by the classical fluctuations and thus help exploring the landscape much better. Ergodicity here means the loss of the memory of the initial state in course of evolution (weak ergodicity) and the convergence to a stationary distribution irrespective of the the initial state (strong ergodicity). The nature of these quantum phase transitions in such systems have also been extensively studied. These studies (Sec. IID) endow one with the knowledge of the phase diagram and the location of the quantum critical point or the phase boundary, which is crucial for choosing the proper quantum kinetic terms and the annealing path (Sec. IIIA and Sec. IIIB).

c) The most natural connection between the paradigm of classical spin glasses and hard optimization problems comes through a widely used and well established optimization technique, namely, simulated annealing algorithm as discussed earlier. The possibility of quantum tunneling through classically impenetrable barriers, as indicated from the studies of quantum spin glasses, naturally suggests an elegant and often more effective alternative to simulated annealing.

In quantum annealing, one has a classical Hamiltonian (or a multivariate cost function viewed as the same) to be optimized, to which, one adds a (non-commuting) quantum kinetic term and reduce it from a very high initial value to zero eventually. This reduction, when done completely adiabatically, assures reaching of the ground state of the classical glass at the end, assuming that there is no crossing of energy levels with the ground state in the course of evolution, and provided that the starting state was the ground state of the initial Hamiltonian. To start with, the tunneling field is much higher than the inter-

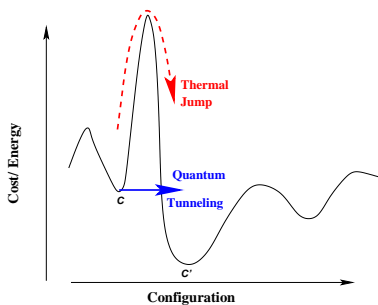


FIG. 1 While optimizing the cost function of a computationally hard problem (like the ground state energy of a spin glass or the minimum travel distance for a traveling salesman problem), one has to get out of a shallower local minimum like the configuration  $C$  (spin configuration or travel route), to reach a deeper minimum  $C'$ . This requires jumps or tunneling like fluctuations in the dynamics. Classically one has to jump over the energy or the cost barriers separating them, while quantum mechanically one can tunnel through the same. If the barrier is high enough, thermal jump becomes very difficult. However, if the barrier is narrow enough, quantum tunneling often becomes quite easy.

action term, so the ground state (a uniform superposition of all classical configurations) is trivially realizable. Simulations clearly demonstrate that quantum annealing can occasionally help reaching the ground state of a complex glassy system much faster than could be done using thermal annealing (discussed later in Sec. III). An experiment comparing the classical and quantum annealing for a spin glass also shows that the relaxations in course of quantum annealing are often much faster than those during the corresponding classical annealing, as discussed in Sec. IIID. What makes quantum annealing fundamentally different from the classical annealing, is the non-local nature (Sec. III) and its higher tunneling ability (Secs. IID & IIIC).

Quantum annealing thus permits a realization of analog quantum computation, which is an independent and powerful complement to digital quantum computation, where discrete unitary transformations are implemented through quantum logic gates.

## II. OPTIMIZATION AND ANNEALING

### A. Combinatorial Optimization Problems

The occurrence of multivariate optimization problems is ubiquitous in our life, wherever one has to choose the best bargain from a host of available options that depend on many independent factors. In many cases, such a task can be cast as a problem of minimizing a given cost or energy function  $\mathcal{H}(S_1, S_2, \dots, S_N)$  with respect to  $N$  variables  $S_1, S_2, \dots, S_N$  (sometimes subject to some constraints). The task is to find a set of values for these variables (a configuration) for which the function  $\mathcal{H}(\{S_i\})$  has the minimum value (cf. Fig. 1). In many important optimization problems, the set of feasible configurations from which an optimum is to be chosen is a finite set (for

finite  $N$ ). In such a case, we say that the problem is combinatorial in nature. If the variables  $S_i$  are discrete and each takes up a finite number of values, then the problem is clearly a combinatorial one. Moreover, certain problems with continuous variables (like linear programming problem) can also be reduced to combinatorial problems (Papadimitriou et al 1998). Here we focus on this type of optimization problem, and assume that we have to minimize  $\mathcal{H}(\{S_i\})$  with respect to the discrete set of the variables  $S_i$ .

An optimization problem is said to belong to the class P (P for Polynomial), if it can be solved in polynomial time (i.e., the evaluation time goes like some polynomial in  $N$ ) using polynomially (in  $N$ , again) bound resources (computer space, processors etc). Existence of such a polynomial bound on the evaluation time is somehow interpreted as the “easiness” of the problem. However, many important optimization problems seem to fall outside this class, like, the famous traveling salesman problem (see Sec. IIC.2).

There is another important class of problems which can be solved in polynomial time by nondeterministic machines. This class is the famous NP (Nondeterministic Polynomial) class (Garey and Johnson 1979). P is included completely in the NP class, since a deterministic Turing machine is just a special case of nondeterministic Turing machines. Unlike a deterministic machine, which takes a specific step deterministically at each instant (and hence follows a single computational path), a nondeterministic machine has a host of different ‘allowed’ steps at its disposal at every instant. At each instant it explores all the ‘allowed’ steps and if any of them leads to the goal, the job is considered to be done. Thus it explores in parallel many paths (whose number goes roughly exponentially with time) and checks if any one of them reaches the goal.

Among the NP problems, there are certain problems (known as NP-complete problems) which are such that any NP problem can be “reduced” to them using a polynomial algorithm. The famous 3-SAT problem (see Sec. IIIA.3) is a representative of the class.

This roughly means that if one has a routine to solve an NP-complete problem of size  $N$  then using that routine one can solve any NP problem at the cost of an extra overhead in time that goes only polynomially with  $N$ . The problems in this class are considered to be hard, since so far no one can simulate a general nondeterministic machine by a deterministic Turing machine (or any sequential computer with polynomially bound resources) without an exponential growth of execution time. In fact it is largely believed (though not proved yet) that it is impossible to do so (i.e.,  $P \neq NP$ ) in principle. However, assuming this to be true, one can show that there are indeed problems in NP class that are neither NP-complete nor P (Garey and Johnson 1979).

## B. Statistical Mechanics of the Optimization Problems and Thermal Annealing

There are some excellent deterministic algorithms for solving certain optimization problems exactly (Papadimitriou and Steiglitz 1998, Hartmann and Rieger, 2002). These algorithms are, however, quite small in number and are strictly problem specific. For NP or harder problems, only approximate results can be found using these algorithms in polynomial time. These approximate algorithms too are also strictly problem specific in the sense that if one can solve a certain NP-complete problem up to a certain approximation using some polynomial algorithm, then that does not ensure that one can solve all other NP problems using it up to the said approximation in polynomial time.

Exact algorithms being scarce, one has to go for heuristics algorithms, which are algorithms based on certain intuitive moves, without any guarantee on either the accuracy or the run time for the worst case instance. However, these algorithms are generally easy to formulate and are quite effective in solving most instances of a the intended problems. A general approach towards formulating such approximate heuristics may be based on stochastic (randomized) iterative improvements. The most preliminary one in this family is the local minimization algorithm. In this algorithm one starts with a random configuration  $C_0$  and makes some local changes in the configuration following some prescription (stochastic or deterministic) to generate a new configuration  $C_1$  and calculates the corresponding change in the cost. If the cost is lowered by the change, then the new configuration  $C_1$  is adopted. Otherwise the old configuration is retained. Then in the next step a new local change is attempted again, and so on. This reduces the cost steadily until a configuration is reached which minimizes the cost locally. This means that no further lowering of cost is possible by changing this configuration using any of the prescribed local moves. The algorithm essentially stops there. But generally in most optimization problems (such as in spin glasses), there occur many local minima in the cost-configuration landscape and they are mostly far above the global minimum (see Fig. 1). It is likely that the algorithm therefore gets stuck in one of them and ends up with a poor approximation. One can then start afresh with some new initial configuration and end up with another local minimum. After repeating this for several times, each time with a new initial configuration, one may choose the best result from them. But much better idea would be to get somehow out of shallow local minima. One can introduce some fluctuations or noise in the process so that the movement is not always towards lower energy configurations, but there is also a finite probability to go to higher energy configurations (the higher the final energy, the lower the probability to move to that), and consequently there appear chances to get out of the shallow local minima. Initially, strong fluctuations are adopted (i.e., the probability to go to higher energy con-

figurations is relatively high) and slowly fluctuations are reduced until finally they are tuned off completely. In the mean time the system gets a fair opportunity to explore the landscape more exhaustively and settle into a reasonably deep cost or energy minimum. Kirkpatrick et al (1983) suggested an elegant way: A fluctuation is implemented by introducing an “artificial” temperature  $T$  into the problem such that the transition probability from a configuration  $C_i$  to a configuration  $C_f$  is given by  $\min\{1, \exp[-\Delta_{if}/T]\}$ , where  $\Delta_{if} = E_f - E_i$ , with  $E_k$  denoting the cost or energy of the configuration  $C_k$ . A corresponding Monte Carlo dynamics is defined, say, based on detailed balance, and the thermal relaxation of the system is simulated. In course of simulation, the noise factor  $T$  is reduced slowly from a very high initial value to zero following some annealing schedule. At the end of the simulation one is expected to end up with a configuration whose cost is a reasonable approximation of the globally minimum one. If the temperature is decreased slow enough, say,

$$T(t) \geq N/\log t, \quad (1)$$

where  $t$  denotes the cooling time and  $N$  the system size, then the global minimum is attained with certainty in the limit  $t \rightarrow \infty$  (Geman and Geman 1984). Even within a finite time and with a faster cooling rate, one can achieve a reasonably good approximation (a crystal with only few defects) in practice. This simulated annealing method is now being used extensively by engineers for devising real-life optimization algorithms. We will refer to this as the classical annealing (CA), to distinguish it from quantum annealing (QA) which employs quantum fluctuations. It is important to note that though in this type of stochastic algorithms the system has many different steps with their respective probabilities at its disposal, it finally takes up a single one, say by tossing coins, and thus finally follow a single (stochastically selected) path. Hence it is not equivalent to a non-deterministic machine, where all the allowed paths are checked in parallel at every time-step.

As has been mentioned already, many combinatorial optimization problems can be cast into the problem of finding the ground state of some classical (spin glass like) Hamiltonian  $H(\{S_i\})$ . One can therefore analyze the problem by using statistical mechanics so as to apply physical techniques like simulated annealing. If one naively takes the number of variables  $N$  as the size, then the entropy and the energy are often found to scale differently with  $N$  and the application of standard thermodynamic arguments become difficult. One needs to scale temperature and some other quantities properly with  $N$  so that one can talk in terms of the concepts like free energy minimization etc. Moreover, the constraints present in the problems are often very difficult to take into account.

## C. Spin Glass and Optimization

### 1. Finding The Ground States of the Classical Spin Glasses

As has been mentioned already, the difficulty faced by a physically motivated optimization heuristic (one that follows physical relaxation dynamics, classical or quantum, to search for the solution), in finding the solution of a hard optimization problem, is similar to that faced by a glassy system in reaching its ground state. In fact, finding the ground states of the spin glasses is an important class of combinatorial optimization problem, which includes an NP-complete problem (Barahona 1982), and many other apparently different ones (like the traveling salesman problem) can be recast in this form. Hence here we discuss very briefly the nature of the spin glass phase and the difficulty in reaching its ground state.

The interaction energy of a typically random and frustrated Ising spin glass (Binder and Young 1986, Nishimori 2001, Dotsenko 2001) may be represented by a Hamiltonian of the form

$$\mathcal{H} = - \sum_{i>j}^N J_{ij} S_i S_j, \quad (2)$$

where  $S_i$  denote the Ising spins and  $J_{ij}$  the interactions between them. These  $J_{ij}$ s here are quenched variables which vary randomly both in sign and magnitude following some distribution  $\rho(J_{ij})$ . The typical distributions are (zero mean) Gaussian distribution of positive and negative  $J_{ij}$  values

$$\rho(J_{ij}) = A \exp\left(\frac{-J_{ij}^2}{2J^2}\right), \quad (3)$$

and binary distribution

$$\rho(J_{ij}) = p\delta(J_{ij} - J) + (1-p)\delta(J_{ij} + J), \quad (4)$$

with probability  $p$  of having a  $+J$  bond, and  $(1-p)$  of having a  $-J$  bond. Two well studied models are the SK model (introduced by Sherrington and Kirkpatrick 1975) and the EA model (introduced by Edward and Anderson 1975). In the SK model the interactions are infinite-ranged and for the sake of extensivity (for rules of equilibrium thermodynamics to be applicable, energy should be proportional to the volume or its equivalent that defines the system-size) one has to scale  $J \sim 1/\sqrt{N}$ , while in the EA model, the interactions are between the nearest neighbors only. For both of them, however,  $\rho(J_{ij})$  is Gaussian;  $A = (N/2\pi J^2)^{1/2}$  for normalization in the SK model.

The freezing (below  $T_c$ ) is characterized by some non-zero value of the thermal average of the magnetization at each site (local ordering). However, since the interactions are random and competing, the spatial average of single-site magnetization (below  $T_c$ ) is zero. Above  $T_c$ ,

both the spatial and the temporal averages of the single-site magnetization of course vanishes. A relevant order parameter for this freezing is therefore

$$q = \frac{1}{N} \overline{\sum_i \langle S_i \rangle_T^2}, \quad (5)$$

(overhead bar denoting the average over disorders (the distribution of  $J_{ij}$ ) and  $\langle \dots \rangle_T$  denotes the thermal average). Here  $q \neq 0$  for  $T < T_c$ , while  $q = 0$  for  $T \geq T_c$ . As will be seen in the following, the existence of a unique order parameter  $q$  will indicate ergodicity.

In the spin glass phase ( $T < T_c$ ), the whole free energy landscape gets divided (cf. Fig. 1) into many valleys (local minima of free energy) separated by very high free energy barriers. Thus the system, once trapped in a valley, remains there for a very long time. The spins of such a confined system are allowed to explore only a very restricted (and correlated) part of the configuration space and thus makes them “freeze” to have a magnetization that characterizes the state (valley) locally.

So far, two competing pictures continue to represent the physics of the spin glasses. The mean-field picture of replica symmetry-breaking is valid for infinite-ranged spin glass systems like the SK spin glass. In this picture, below the glass transition temperature  $T_c$ , the barriers separating the valleys in the free energy landscape actually diverge (in the limit  $N \rightarrow \infty$ ), giving rise to a diverging timescale for the confinement of the system in any such valley once the system gets there somehow. This means there is a loss of ergodicity in the thermal dynamics of the system at  $T < T_c$ . Thus one needs a distribution  $P(q)$  of order parameters, instead of a single order parameter to characterize the whole landscape, as emerges naturally from the replica symmetry-breaking ansatz of Parisi (1980). To be a bit more quantitative, let us imagine that two identical replicas (having exactly the same set  $J_{ij}$ s) of a spin glass sample are allowed to relax thermally below  $T_c$ , starting from two different random (paramagnetic) initial states. Then these two replicas (labeled by  $\mu$  and  $\nu$ , say) will settle in two different valleys, each being characterized by a local value of the order parameter and the corresponding overlap parameters  $q_{\mu\nu}$  having a sample-specific distribution

$$P_J(q) = \sum_{\mu,\nu} e^{-\frac{F_\mu + F_\nu}{T}} \delta(q - q_{\mu\nu});$$

$$P(q) = \int \prod_{i>j} dJ_{ij} \rho(J_{ij}) P_J(q). \quad (6)$$

Here the subscript  $J$  denotes a particular sample with a given realization of quenched random interactions ( $J_{ij}$ s) between the spins, and finally averaging  $P_J(q)$  over disorder distribution  $\rho(J)$  in (2) or (3) one gets  $P(q)$ . Physically,  $P(q)$  gives the probability distribution for the two pure states to have an overlap  $q$ , assuming that the probability of reaching any pure state  $\mu$  starting from a random

(high temperature) state is proportional to the thermodynamic weight  $\exp\{-F_\mu\}$  of the state  $\mu$ . The other picture is due to the droplet model of short-range spin glass (Bray and Moore 1984, Fisher and Huse 1986), where there is no divergence in the typical free energy barrier height and the relevant timescale is taken to be that of crossing the free energy barrier of formation of a typical droplet of same (all up or all down) spins. Based on certain scaling ansatz, this picture leads to a logarithmically decaying (with time) self-correlation function for the spins below the freezing temperature  $T_c$ .

The issue of the validity of the mean-field picture (of the replica symmetry-breaking) in the context of the real-life spin glasses, where the interactions are essentially short-range, is far from settled (see e.g., Moore et al 1998, Marinari et al 1998, Krzakala et al 2001 and Gavriro et al 2006). However, the effective Hamiltonian (cost function) for many other optimization problems may contain long-range interactions and may even show the replica symmetry-breaking behavior shown in the Graph Partitioning Problem (Fu and Anderson 1986). Of course, no result of QA for such system (for which replica symmetry-breaking is shown explicitly) has been reported yet. The successes of QA reported so far are mostly for short-range systems. Thus, the scope of quantum annealing in those long-range systems still stands out as an interesting open question.

## 2. The Traveling Salesman Problem

In the traveling salesman problem (TSP), there are  $N$  cities placed randomly in a country having a definite metric to calculate the inter-city distances. A salesman has to make a tour to cover every city and finally come back to the starting point. The problem is to find a tour of minimum length. An instance of the problem is given by a set  $\{d_{ij}; i, j = 1, N\}$ , where  $d_{ij}$  indicates the distance between the  $i$ -th and the  $j$ -th city, or equivalently, the cost for going from the former to the later. We mainly focus on the results of symmetric case, where  $d_{ij} = d_{ji}$ . The problem can be cast into the form where one minimizes an Ising Hamiltonian under some constraints, as shown below. A tour can be represented by an  $N \times N$  matrix  $\mathbf{T}$  with elements either 0 or 1. In a given tour, if the city  $j$  is visited immediately after visiting city  $i$ , then  $\mathbf{T}_{ij} = 1$ , or else  $\mathbf{T}_{ij} = 0$ . Generally an additional constraint is imposed that one city has to be visited once and only once in a tour. Any valid tour with the above restriction may be represented by a  $\mathbf{T}$  matrix whose each row and each column has one and only one element equal to 1 and rest all are 0s. For symmetric a metric, a tour and its reverse tour have the same length, and it is more convenient to work with an undirected tour matrix  $\mathbf{U} = \frac{1}{2}(\mathbf{T} + \hat{\mathbf{T}})$ , where  $\hat{\mathbf{T}}$ , the transpose of  $\mathbf{T}$ , represents the reverse of the tour given by  $\mathbf{T}$ . Clearly,  $\mathbf{U}$  must be a symmetric matrix having two and only two distinct entries equal to 1 in every row and every column, no two

rows being identical, and so is not any two columns. In terms of  $\mathbf{U}_{ij}$ s, the length of a tour can be represented by

$$\mathcal{H} = \frac{1}{2} \sum_{i,j=1}^N d_{ij} \mathbf{U}_{ij}. \quad (7)$$

One can rewrite the above Hamiltonian in terms of Ising spins  $S_{ij}$ s as

$$\mathcal{H}_{TSP} = \frac{1}{2} \sum_{i,j=1}^N d_{ij} \frac{(1 + S_{ij})}{2} \quad (8)$$

where  $S_{ij} = 2\mathbf{U}_{ij} - 1$  are the Ising spins. The Hamiltonian is similar to that of a non-interacting Ising spins on an  $N \times N$  lattice, with random fields  $d_{ij}$  on the lattice points  $\{i, j\}$ . The frustration is introduced by the global constraints on the spin configurations in order to conform with the structure of the matrix  $\mathbf{U}$  discussed above. The problem is to find the ground state of the Hamiltonian subject to these constraints. There are  $N^2$  Ising spins, which can assume  $2^{N^2}$  configurations in absence of any constraint, but the constraint here reduces the number of valid configurations to that of the number of distinct tours, which is  $(N!)/2N$ .

Mainly two distinct classes of TSP are studied: one with an Euclidean  $d_{ij}$  in finite dimension (where  $d_{ij}$  are strongly correlated through triangle inequalities, which means, for any three cities  $A, B$  and  $C$ , the sum of any two of the side  $AB, BC$  and  $CA$  must be greater than the remaining one), and the other with random  $d_{ij}$  in infinite dimension.

In the first case,  $N$  cities are uniformly distributed within a hypercube in a  $d$ -dimensional Euclidean space. Finding a good approximation for large  $N$  is easier for this case, since the problem is finite-ranged. Here a  $d$ -dimensional neighborhood is defined for each city, and the problem can be solved by dividing the whole hypercube into a number of smaller pieces and then searching for the least path within each smaller part and joining them back. The correction to the true least path will be due to the unoptimized connections across the boundaries of the subdivisions. For a suitably made division (not too small), this correction will be of the order of the surface-to-volume ratio of each division, and thus will tend to zero in the  $N \rightarrow \infty$  limit. This method, known as “divide and conquer”, forms a reasonable strategy for solving approximately such finite-range optimization problems (including finite-range spin glasses) in general. In the second case,  $d_{ij}$ s are assigned completely randomly, with no geometric (e.g., Euclidean) correlation between them. The problem in this case becomes more like a long-range spin glass. A self avoiding walk representation of the problem was made using an  $m$ -component vector field, and the replica analysis was done (Mezard et al 1987) for finite temperature, assuming replica symmetry ansatz to hold. Moreover, true breaking of ergodicity may occur only in infinite systems, not in any finite instance of the problem. The results, when extrapolated to

zero-temperature, do not disagree much with the numerical results (Mezard et al 1987). The stability of a replica symmetric solution has not yet been proved for low temperature region. However, numerical results of thermal annealing for instances of size  $N = 60$  to  $N = 160$  yielded many near optimal tours, and the corresponding overlap analysis shows a sharply peaked distribution, whose width decreases steadily with increase in  $N$ . This indicates the existence of a replica symmetric phase for the system (Mezard et al 1987).

An analytical bound on the average (Normalized by  $N^{1/2}$ ) value of optimal path-length per city ( $\Omega$ ) calculated for TSP on 2-dimensional Euclidean plane has been found to be  $5/8 < \Omega < 0.92$  (Bearwood et al 1959). Careful scaling analysis of the numerical results obtained so far indicates the lower bound to be close to 0.72 (Percus and Martin 1996, Chakraborti and Chakrabarti 2000).

Simulated (thermal) annealing of a Euclidean TSP on a square having length  $N^{1/2}$  (so as to render the average nearest neighbor distance independent of  $N$ ) has been reported (Kirkpatrick et al 1983). In this choice of length unit, the optimal tour length per step ( $\Omega$ ) becomes independent of  $N$  for large  $N$ . Thermal annealing rendered  $\Omega \leq 0.95$  for  $N$  up to 6000 cities. This is much better than what is obtained by the so called “greedy heuristics”, (where being at some city in a step, one moves to the nearest city not in the tour in the next step) for which  $\Omega \sim 1.12$  on average. Later we will see that (Sec. IIIA) that quantum annealing can do even better than thermal annealing in context of random TSP.

To summarize, when cast in some energy minimization problem, the combinatorial optimization problems may exhibit glassy behavior during thermal annealing. Even replica symmetry-breaking behavior may be observed (like in case of Graph Partitioning Problem, see Fu and Anderson 1986), since the underlying Hamiltonian need not be short-range, and the constraints can bring frustrations into the problem. One can intuitively conclude that thermal annealing or other heuristics would not be able to solve such problems easily to a good approximation within reasonable time. Moreover, practically nothing can be said about the time required to solve the worst case instance exactly. Specifically, in some cases, where good solutions are thermodynamically very insignificant in number and there is no monotonic gradient towards them, the entropy might make a classical search exponentially difficult, though the landscape might still remain completely ergodic. Later we will see quantum searches can bring about spectacular improvements in some such cases (see Sec. IIIB and Fig. 4).

#### D. Quantum Spin Glasses and Annealing

In QA one adds a kinetic (tunneling) term to the interaction part of the classical glass Hamiltonian. The object that results in, is called a quantum spin glass. The knowledge of the phase-diagram of a quantum spin glass

is crucially important for its annealing, as it gives an idea of the location of the quantum critical points on the phase diagram, and thus offers a guideline to choose the proper kinetic terms (that maintain a sizable gap) and the suitable annealing paths (see Sec. IIIA and IIIB).

In quantum spin glasses (Chakrabarti 1981, Ishii and Yamamoto 1985, Bhatt 1998, Rieger 2005, Sachdev 1999, Ye 1993), the order-disorder transition (i.e., from the frozen phase to the high kinetic energy phase, termed the para phase) can be driven both by thermal fluctuations as well as by quantum fluctuations. Quantum spin glasses can be of two types: vector spin glasses, where the quantum fluctuations cannot be adjusted by changing some laboratory field, and the other, a classical spin glass perturbed by some quantum tunneling term, where the quantum fluctuations are controlled through, say, a transverse laboratory field.

The amount of the quantum fluctuations being adjustable, this transverse Ising spin glass (TISG) model is perhaps the simplest model in which the quantum effects in a random system can be and have been studied extensively and systematically (Chakrabarti et al 1996). Here we will focus only on TISG, since the reduction of the quantum fluctuations is the key feature required for quantum annealing.

The interest in the zero-temperature quantum spin glass phases in the TISG models have been been complimented all along by the experimental studies in several systems which have been established to be represented accurately by transverse field Ising model (TIM). Recent discovery of the compound material  $\text{LiHo}_x\text{Y}_{1-x}\text{F}_4$  with the magnetic Ho ion concentration  $x = 0.167$  (Aeppli and Rosenbaum 2005, Wu et al 1991, Wu et al 1993a) representing accurately a random long-range transverse Ising system, has led to renewed interest. Here, the strong spin-orbit coupling between the spins and the host crystals restricts the effective “Ising” spins to align either parallel or anti-parallel to the specific crystal axis. An applied magnetic field, transverse to the preferred axis, flips the “Ising” spins. This feature, together with the randomness in the spin-spin interaction, makes it a unique TISG-like system. Most interestingly, it has been shown that in spite of the presence of all the three ingredients - frustrations, randomness and the long-range (dipolar) interactions, that are necessary for the formation of a spin glass, the spin glass phase of  $\text{LiHo}_x\text{Y}_{1-x}\text{F}_4$  is actually destroyed by any finite transverse field (Schechter and Lafflorencie 2006). This indicates the effectiveness of quantum tunneling in the exploration of a rugged PEL with formidable potential energy barriers. The TISG model described here, is given by the Hamiltonian

$$\mathcal{H} = - \sum_{i>j}^N J_{ij} S_i^z S_j^z - \Gamma \sum_i^N S_i^x, \quad (9)$$

where  $\Gamma$  denotes the tunneling strength at each site and  $J_{ij}$ s are distributed randomly following the distribution

$\rho(J_{ij})$  given by (3) or (4). Generally, we denote the strength of the quantum kinetic term by  $\Gamma$ .

The unique interest in such quantum spin glass system comes from the possibility of much faster crossing of the high barriers occurring in the potential energy landscapes of the classical spin glasses by means of quantum tunneling induced by the transverse field, compared to that done thermally by scaling such barriers with the temperature.

The phase transitions in quantum spin glasses can be driven both by thermal and quantum fluctuations as mentioned before and the equilibrium phase diagrams also indicate how the optimized solution (in SG phase) can be obtained either by tuning of the temperature  $T$  or the tunneling field  $\Gamma$ , or by both. We will show later (in context of quantum annealing) that reaching the phase by tuning  $\Gamma$  may often be more advantageous (faster) than that by tuning  $T$ .

The short-range version of this TISG model was first studied by Chakrabarti (1981), and the long-range version, discussed here, was first studied by Ishii and Yamamoto (1985). Several analytical studies have been made to obtain the phase diagram of the transverse Ising SK model (Miller and Huse 1993). The problem of an SK glass in a transverse field becomes a nontrivial one due to the presence of non-commuting spin operators in the Hamiltonian. This leads to a dynamical frequency-dependent self-interaction for the spins.

One can study an effective-spin Hamiltonian for the SK model in a transverse field within the mean field framework very easily. The spin glass order parameter in a classical SK model is given by a random ‘mean field’  $h(r)$  having Gaussian distribution (see Binder and Young 1986)

$$q = \int_{-\infty}^{+\infty} dr e^{-r^2/2} \tanh^2(h^z(r)/T); \quad h^z(r) = J\sqrt{q}r + h^z \quad (10)$$

where  $h^z$  denotes the external field (in  $z$  direction), the mean-field  $h(r)$  being also in the same direction. In the presence of the transverse field, as in (9),  $h(r)$  has components both in  $z$  and  $x$  directions

$$\vec{h}(r) = -h^z(r)\hat{z} - \Gamma\hat{x}; \quad h(r) = \sqrt{h^z(r)^2 + \Gamma^2}, \quad (11)$$

and one replaces the ordering term  $\tanh^2(h(r)/T)$  in (10) by its component  $[|h^z(r)|/|h(r)|]^2 \tanh^2(|h(r)|/T)$  in the  $z$ -direction. Putting  $h^z = 0$  and  $q \rightarrow 0$  one gets the phase boundary equation as (see Chakrabarti et al 1996)

$$\frac{\Gamma}{J} = \tanh\left(\frac{\Gamma}{T}\right). \quad (12)$$

This gives  $\Gamma_c$  ( $T = 0$ ) =  $J = T_c$  ( $\Gamma = 0$ ) and a phase diagram qualitatively similar to the experimental one shown in Fig. 2.

Several Monte Carlo studies have been performed for the SK spin glass model in transverse field applying the Suzuki-Trotter formalism (see Appendix 1), mapping a

$d$ -dimensional quantum Hamiltonian to an effective  $d+1$  dimensional anisotropic classical Hamiltonian (see also Hatano and Suzuki 2005). The partition function gives the effective classical Hamiltonian in the  $M$ th Trotter approximation as

$$\mathcal{H} = \sum_{i>j}^N \sum_k^M K_{ij} S_{ik} S_{jk} - \sum_i^N \sum_k^M K S_{ik} S_{ik+1}, \quad (13)$$

with

$$K_{ij} = \frac{J_{ij}}{MT}; \quad K = \frac{1}{2} \ln \coth\left(\frac{\Gamma}{MT}\right), \quad (14)$$

where  $S_{ik}$  denotes the Ising spin defined on the lattice site  $(i, k)$ ,  $i$  denoting the position in the original SK model and  $k$  denoting the position in the additional Trotter dimension. Although the equivalence between classical and the quantum model holds exactly in the limit  $M \rightarrow \infty$ , one can always make an optimum choice for  $M$ . The equivalent classical Hamiltonian has been studied using standard Monte Carlo technique. The numerical estimates of the phase diagram etc. are reviewed in details in (Bhatt 1998, Rieger 2005). Ray et al (1989) took  $\Gamma \ll J$  and their results indeed indicated a sharp lowering of  $T_c(\Gamma)$ . Such sharp fall of  $T_c(\Gamma)$  with large  $\Gamma$  is obtained in almost all the theoretical studies of the phase diagram of the model (Miller and Huse 1993; Ye et al 1993; see also Bhatt 1998 and Rieger 2005). Quantum Monte Carlo (Alvarez and Ritort 1996) as well as real-time Schrödinger evolution (the true dynamics given by the time-dependent Schrödinger equation) studies of SK spin glass in transverse field were made (Lancaster and Ritort, 1997).

In the Hamiltonian for the EA spin glass in presence of a transverse field, given by (9), the random interactions are restricted among the nearest neighbors and satisfy a Gaussian distribution with zero mean and variance  $J$ , as given by Eq. (3). Here, the variation of correlations in the equivalent  $(d+1)$  dimensional classical model fitted very well (Guo et al 1994) with the scaling fit with a unique order parameter and a critical interval corresponding to a phase diagram whose features are similar to those discussed above (see also Chakrabarti et al 1996, Bhatt 1998 and Rieger 2005).

As discussed earlier in this section,  $\text{LiHo}_x\text{Y}_{1-x}\text{F}_4$  with  $x = 0.167$  provides a spin glass system, for which the external magnetic field transverse to the preferred axis scales like the square root of the tunneling field  $\Gamma$  in (9). With increasing transverse field, the glass transition temperature decrease monotonically, as shown in Fig. 2.

A quantum tunneling term allows for overlap between two classically localized states and the dynamics near the ground states of such glasses show better ergodicity properties. In order to investigate this aspect of quantum spin glasses, one can study the overlap distribution function  $P(q)$  given by (6). If the ergodicity is recovered, at least for a part of the phase diagram, the above function



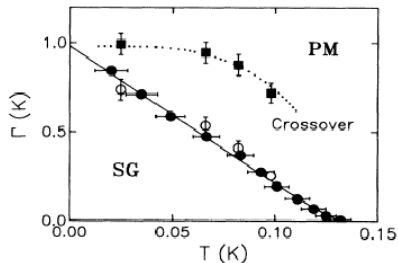


FIG. 2 Phase diagram of  $\text{LiHo}_{0.167}\text{Y}_{0.833}\text{F}_4$  according to the dynamical measurements (filled circles) and of the nonlinear susceptibility measurements (open circles). Filled squares indicate the freezing boundary obtained from AC susceptibility measurements (taken from Wu et al 1993b).

should tend to a delta function form, peaking at some finite value of the order-parameter  $q$  in thermodynamic limit. In the para-phase, of course, the distribution becomes a delta function at  $q = 0$  for the infinite system. In spite of several investigations (see e.g., Ray et al 1989, Thirumalai and Kirkpatrick 1989, Goldschmidt and Lai 1990, Chakrabarti et al 1996, Kim and Kim 2002) the point of replica symmetry restoration in spin glasses by quantum fluctuation is not settled yet. However, slow withdrawal (see Eq. 16 for the characteristic slowness) of the tunneling field in these quantum spin glasses can help annealing the system close to the ground state of the classical spin glass eventually, as has been described in the next section.

### III. QUANTUM ANNEALING

In the previous sections we have seen how thermal fluctuations can be utilized to devise fast heuristics to find an approximate ground state of a glassy system, or equivalently, a near-optimal solution to combinatorial problem, whose cost-configuration landscape has glassy behavior due to the occurrence of many local minima. There are two aspects of an optimization problem which might render thermal annealing to be a very ineffective one. First, in a glassy landscape, there may exist very high cost/energy barriers around local minima which does not correspond to a reasonably low cost (see Fig. 1). In the case of infinite-range problems, these barriers might be proportional to the system-size  $N$ , and thus diverge in thermodynamic limit. Thus there might occur many unsatisfactory local minima, any of which can trap the system for very long time (which actually diverges in thermodynamic limit for infinite-range systems) in course of annealing. The second problem is the entropy itself. The number of configurations grow very fast with the number of variables (roughly exponentially;  $n$  Ising spin can be in  $2^n$  configurations) and a classical system can only assume one configuration at a time and unless there is a gradient that broadly guides the system towards the global minimum from any point in the configuration space, the

search has to involve visiting any substantial fraction of the configurations. Thus a PEL without a guiding gradient poses a problem which is clearly of an exponential or higher order in complexity (depending how the size of the configuration space scales with the system-size  $N$ ), and the CA algorithms can do no better than a random search algorithm. This is the case for golf-course type potential-energy landscape (where there is a sharp potential minimum on completely flat PEL) (see Sec. IIIB, Fig. 4). One can imagine that quantum mechanics might have some solutions to both these problems, at least, to some extent.

This is because quantum mechanics can introduce classically unlikely tunneling paths even through very high barriers if they are narrow enough (Ray et al 1989). This can solve the ergodicity problem to some extent, as discussed earlier. Even in places where ergodicity breaking does not take place in true sense, once the energy landscape contains high enough barriers (specially for infinite-ranged quenched interactions), quantum tunneling may provide much faster relaxation to the ground state (Santoro et al 2002, Martoňák et al 2002).

In addition, a quantum mechanical wave function can delocalize over the whole configuration space (i.e., over the potential energy landscape) if the kinetic energy term is high enough. Thus it can actually “see” the whole landscape simultaneously at some stage of annealing.

These two aspects can be expected to improve the search process when employed properly. In fact such improvements can indeed be achieved in certain situations, though quantum mechanics is not a panacea for all such diseases as ergodicity breaking, spin glass behavior etc, and certainly has its own inherent limitations. What intrigues one is the fact that the limitations due to quantum nature of an algorithm are inherently different from those faced by its classical counterpart, and thus it is not yet clear in general which wins when. Here we discuss some results regarding the quantum heuristics and some of their general aspects understood so far. For more detailed reviews of the subject we refer to the articles in Das and Chakrabarti (2005) and Santoro and Tosatti (2006).

Some basic aspects of QA can be understood from the simple case of QA in the context of a double-well potential (Stella 2005, Battaglia et al 2005). Typically a particle in a double-well consisting of a shallower but wider well and a deeper but narrower well is annealed (it is likely that the deeper well, i.e., the target state, is narrower, otherwise the searching becomes easier even classically). The kinetic energy (inverse mass) is tuned from a very high value to zero linearly within a time  $\tau$ . For a very high value of initial kinetic energy, the wave function, which is the ground state, is delocalized more or less over the whole double-well. As kinetic energy is reduced but still quite high, the ground state corresponds to a more pronounced peak on the shallower minimum, since it is wider. This is because at this stage, to obtain the minimal (ground state) energy, it is more effective to minimize the kinetic energy by localization over a wider

space, rather than minimizing the potential energy by localizing in the deeper well. However, as kinetic energy is tuned down further, the potential energy term becomes dominating, and the ground state has a taller peak around the deeper minimum. The evolving wave function can roughly follow this ground state structure all the way and finally settle to the deeper minimum if the annealing time  $\tau$  is greater than some  $\tau_c$ . When  $T < T_c$  it fails to tunnel from its early state localized in the shallower well to the deeper well as the kinetic energy is decreased. This result is qualitatively the same for both real-time and quantum Monte Carlo annealing, excepting for the fact that the  $\tau_c$ 's are different in the two cases.

The realization of QA consists of employing adjustable quantum fluctuations into the problem instead of a thermal one (Kadowaki and Nishimori 1998, Amara et al 1993, Finnila et al 1994). In order to do that, one needs to introduce an artificial quantum kinetic term  $\Gamma(t)\mathcal{H}_{kin}$ , which does not commute with the classical Hamiltonian  $\mathcal{H}_C$  representing the cost function. The coefficient  $\Gamma$  is the parameter which controls the quantum fluctuations. The total Hamiltonian is thus given by

$$\mathcal{H}_{tot} = \mathcal{H}_C + \Gamma(t)\mathcal{H}_{kin}. \quad (15)$$

The ground state of  $\mathcal{H}_{tot}$  is a superposition of the eigenstates of  $\mathcal{H}_C$ . For a classical Ising Hamiltonian of the form (2), the corresponding total quantum Hamiltonian might have the form (9), where  $\mathcal{H}_C = -\sum_{i>j} i^N S_i^z S_j^z$  and  $\mathcal{H}_{kin} = -\sum_i^N S_i^x$ . Initially  $\Gamma$  is kept very high so that the  $\mathcal{H}_{kin}$  dominates and the ground state is trivially a uniform superposition of all the classical configurations. One starts with that uniform superposition as the initial state, and slowly decreases  $\Gamma$  following some annealing schedule, eventually to zero. If the process of decreasing is slow enough, the adiabatic theorem of quantum mechanics (Sarandy et al 2004) assures that the system will always remain at the instantaneous ground state of the evolving Hamiltonian  $\mathcal{H}_{tot}$ . When  $\Gamma$  is finally brought to zero,  $\mathcal{H}_{tot}$  will coincide with the original classical Hamiltonian  $\mathcal{H}_C$  and the system will be found in the ground state of it, as desired. The special class of QA algorithms, where strictly quasi-stationary or adiabatic evolutions are employed are also known as Quantum Adiabatic Evolution algorithms (Farhi et al 2001).

Two important questions are how to choose an appropriate  $\mathcal{H}_{kin}$  and how slow the evolution needs to be in order to assure adiabaticity. According to the adiabatic theorem of quantum mechanics, for a non-degenerate spectrum with a gap between the ground state and first excited state, the adiabatic evolution is assured if the evolution time  $\tau$  satisfies the following condition-

$$\tau \gg \frac{|\langle \dot{\mathcal{H}}_{tot} \rangle|_{max}}{\Delta_{min}^2}, \quad (16)$$

where

$$|\langle \dot{\mathcal{H}}_{tot} \rangle|_{max} = \max_{0 \leq t \leq \tau} \left[ \left| \left\langle \phi_0(t) \left| \frac{d\mathcal{H}_{tot}}{ds} \right| \phi_1(t) \right\rangle \right| \right],$$

$$\Delta_{min}^2 = \min_{0 \leq t \leq \tau} [\Delta^2(t)]; \quad s = t/\tau; \quad 0 \leq s \leq 1, \quad (17)$$

$|\phi_0(t)\rangle$  and  $|\phi_1(t)\rangle$  being respectively the instantaneous ground state and the first excited state of the total Hamiltonian  $\mathcal{H}_{tot}$ , and  $\Delta(t)$  the instantaneous gap between the ground state and the first excited state energies (see Sarandy et al 2004). One may wonder that while entering the ordered phase ( $\Gamma < \Gamma_c$ ) from the para phase ( $\Gamma > \Gamma_c$ ) in course of annealing, the gap  $\Delta$  may vanish at the phase boundary ( $\Gamma = \Gamma_c$ ) in the  $N \rightarrow \infty$  limit. In fact, in such a case, QA cannot help anyway in finding the ground state of an infinite system. However, for any finite sample, this gap is very unlikely to vanish for a random system, and QA may still work out nicely.

However, it is impossible to follow, even for a finite  $N$ , the evolution of a full wave function in a classical computer using polynomial resources in general, since it requires tracking the amplitudes of all the basis vectors (all possible classical configurations), whose number grows exponentially with system-size  $N$ . Such an adiabatic evolution may be realized within polynomial resources only if one can employ a quantum mechanical system itself to mimic the dynamics. However, one may employ quantum Monte Carlo methods to simulate some dynamics (not the real-time quantum dynamics) to sample the ground state (or a mixed state at low enough temperature) for a given set of parameter values of the Hamiltonian. Annealing is done by reducing the strength  $\Gamma$  of the quantum kinetic term in the Hamiltonian from a very high value to zero following some annealing schedule in course of simulation. In case of such Monte Carlo annealing algorithm, there is no general bound on success time  $\tau$  like the one provided by the adiabatic theorem for true Schrödinger evolution annealing. Here we will separately discuss the results of real-time QA and Monte Carlo QA. Apart from these quasi-stationary quantum annealing strategies, where the system always stays close to some stationary state (or low-temperature equilibrium state), there may be cases where quantum scatterings (with tunable amplitudes) are employed to anneal the system (Das et al 2005).

## A. Quantum Monte Carlo Annealing

In quantum Monte Carlo annealing, one may employ either a finite (but low) temperature algorithm, or a zero-temperature algorithm. Most of the Monte Carlo QA (Das and Chakrabarti 2005, Santoro and Tosatti 2006) are done using a finite temperature Monte Carlo, namely, the Path Integral Monte Carlo (PIMC), since its implementation is somewhat simpler than that of other zero-temperature Monte Carlo methods .

Among the other zero-temperature Monte Carlo methods used for annealing are the zero-temperature transfer-matrix Monte Carlo (The chapter by Das and Chakrabarti in Das and Chakrabarti, 2005) and the Green's function Monte Carlo (Santoro and Tosatti

2006). However, these algorithms suffer severely from different drawbacks, which renders them much slower than PIMC algorithms in practice.

The Green's function Monte Carlo effectively simulates the real-time evolution of the wave function during annealing. But to perform sensibly, it often requires a guidance that depends on a priori knowledge of the wave function. Without this guidance it may fail miserably (Santoro and Tosatti 2006). But such a priori knowledge is very unlikely to be available in the case of random optimization problems, and hence so far the scope for this algorithm seems to be very restricted.

The zero-temperature transfer-matrix Monte Carlo method, on the other hand, samples the ground state of the instantaneous Hamiltonian (specified by the given value of the parameters at that instant) using a projective method, where the Hamiltonian matrix itself (a suitable linear transformation of the Hamiltonian that converts into a positive matrix, in practice) is viewed as the transfer-matrix of a finite-temperature classical system of one higher dimension (Das and Chakrabarti 2005). But the sparsity of the Hamiltonian matrix for systems with local kinetic terms leaves the classical system highly constrained and thus very difficult to simulate efficiently for large system sizes.

The PIMC has so far been mostly used for QA. The basic idea of path-integral Monte Carlo rests on Suzuki-Trotter formalism (see Appendix 1), which maps the partition function of a  $d$ -dimensional quantum Hamiltonian  $\mathcal{H}$  to that of an effective classical Hamiltonian  $\mathcal{H}_{eff}$  in  $(d+1)$ -dimension. Quantum annealing of a Hamiltonian  $\mathcal{H}_{tot}$  using PIMC consists of mapping  $\mathcal{H}_{tot}$  to its equivalent classical one and simulate it at some fixed low temperature so that thermal fluctuations are low. The quantum fluctuations are reduced from some very high initial value to zero finally through reduction of  $\Gamma$  in course of simulation. Clearly, the simulation dynamics is not the true Schrödinger evolution of the system, and also it cannot simultaneously see the whole configuration space as does a delocalized wave function. It feels the landscape locally and makes moves just like a classical system. The first attempt of quantum annealing using PIMC was done by Kadowaki and Nishimori (1998) for solving TSP and an extensive use of the technique to explore multitude of problems has been made by the group of Santoro and Tosatti (2006). Here we will discuss some PIMC quantum annealing results briefly for few different systems.

### 1. A Short-Range Spin Glass

Quantum annealing of an EA spin glass in 2-dimension (square lattice) using transverse field (see Eq. (9)) for large lattice size (up to  $80 \times 80$ ) using PIMC turns out to be much more efficient compared to thermal annealing (CA) of the same system in finding the approximate ground state (Santoro et al 2002, Martoňák et al 2002). The quantity which is measured is the resid-

ual energy  $\epsilon_{res}(\tau) = E(\tau) - E_0$ ,  $E_0$  being the true ground state energy of the finite system (calculated by the Spin Glass Server using the so called Branch-and-Cut algorithms; see <http://www.informatik.uni-koeln.de/lj;uenger/research/spinglass/>) and  $E(\tau)$  being the final energy of the system after reducing the transverse field strength  $\Gamma$  linearly within time  $\tau$  from some suitably large initial value to zero. Here  $\tau$  is a fictitious time given by the number of Monte Carlo steps.

Classically, for a large class of frustrated disordered system it can be shown, using very general arguments that the residual energy decreases following some power law in the logarithm of the annealing time  $\tau$ , namely,  $\epsilon_{res} \sim (\log \tau)^{-\zeta}$ , with  $\zeta \leq 2$  (Huse and Fisher 1986). In PIMC, the partition function of a  $d$ -dimensional quantum system is mapped to an equivalent  $d+1$ -dimensional classical system (known as Suzuki-Trotter mapping). The effective  $d+1$ -dimensional system, is obtained by replicating the classical part of the original system (say, the Ising interaction part of the transverse Ising system without the transverse field term) with all its interactions (including the disorders) intact along the extra higher dimension. The coupling between the spin in different replica depends on the quantum kinetic term in the original  $d$ -dimensional system.

However, the PIMC annealing results show that the quantum effect (taken into account through Suzuki-Trotter mapping) does not change the basic relaxation behavior of  $\epsilon_{res}(\tau)$ . But still a dramatic improvement in evaluation time is achieved since it turns out that the value of the exponent  $\zeta$  can be much higher ( $\zeta = 6$ ) for QA than the Huse-Fisher bound of  $\zeta \leq 2$  for classical annealing. This is a tremendous improvement in computational time if one thinks in terms of the changes in  $\tau$  required to improve  $\epsilon_{res}$  equally by some appreciable factor in the respective cases of classical and quantum annealing. An interesting asymptotic comparison for results of QA and CA for an  $80 \times 80$  lattice shows that to reach a certain value of  $\epsilon_{res}$ , the PIMC-QA would take one day of CPU time (for the computer used) whereas CA would take about 30 yrs (Santoro et al 2002, Martoňák et al 2002). The result would not be much different in this case if the real-time Schrödinger evolution would have been followed, as has been argued using the Landau-Zener cascade tunneling picture (Santoro et al 2002, Martoňák et al 2002).

Landau-Zener tunneling theory gives an estimate of the probability of tunneling non-adiabatically from a lower to a higher level when the system encounters an avoided level crossing between the levels during time evolution. Let the gap between two energy levels  $|a(t)\rangle$  and  $|b(t)\rangle$  of a time-dependent Hamiltonian vary linearly with time (gap  $\Delta = \alpha t$ ) and encounter an avoided level crossing. Here the levels are energy levels of the classical part of the Hamiltonian (say, the potential energy levels of an Ising model). Let the system be made to evolve in such a way that the characteristic time it spends while passing through the crossing region is  $\tau$ . Let there be a quantum

tunneling field  $\Gamma$  that induces transitions between the levels. Then if the system evolved is at the lower branch  $|a\rangle$  before encountering the avoided level crossing, the probability that it tunnels to the higher branch  $|b\rangle$  while passing through the crossing decreases with the time  $\tau$  as  $P(\tau) = \exp(-\tau/\tau_\Gamma)$ , where  $\tau_\Gamma = (\hbar\alpha\Gamma)/(2\pi\Delta_{min}^2)$ ,  $\Delta_{min}$  being the minimum value of the gap attained at the avoided level crossing. For spin glass-like systems with non-zero gap, treating multiple level-crossings, each with small  $\Delta$ , as a cascade of independent Landau-Zener tunneling, one may argue that residual energy goes as  $\epsilon_{res} \sim (\log \tau)^{-\zeta_Q}$ , where  $\zeta_Q$  is essentially greater than the bound  $\zeta \leq 2$  for thermal annealing, and might be as high as 6 (Santoro et al 2002, Martoňák et al 2002).

## 2. The Traveling Salesman Problem

Quantum annealing of TSP with a random metric (i.e., the distance  $d_{ij}$  between the  $i$ -th and the  $j$ -th city is chosen randomly) in infinite dimension using PIMC was also found to be more efficient than CA in finding an approximately minimal tour (Martoňák et al 2004). An  $N$ -city tour in a random TSP problem can be represented by a configuration of  $N^2$  constrained Ising spins, and the tour length, i.e., the  $\mathcal{H}_c$ , by the Hamiltonian (8). Now to do the annealing, one needs to introduce a set of moves (spin flip operations) that satisfies the constraints. Classically one very important class of moves is the 2-opt moves, which starting from a valid tour, can generate all possible tours without generating any invalid link. Let a valid tour contains two links  $i \rightarrow j$  and  $k \rightarrow l$ . A 2-opt move may consist of removing those two links and establishing the following links:  $i \rightarrow k$  and  $j \rightarrow l$  (here  $i$  denotes  $i$ -th city). Classical annealing of the Hamiltonian can be done by restricting the Monte Carlo moves within 2-opt family only. However, for the quantum case, one needs to design a special transverse field (non-commuting spin-flip term) to enforce the constraints. It can be realized by a spin-flip term of the form  $S_{<k,i>}^+ S_{<l,j>}^+ S_{<j,i>}^- S_{<l,k>}^-$ , where the operator  $S_{i,j}^-$  flips down ( $+1 \rightarrow -1$ ) the Ising spins  $S_{ij}^z$  and  $S_{ji}^z$  when they are in  $+1$  state, and similarly for the flip-up operators  $S_{i,j}^+$ . However, to avoid the Suzuki-Trotter mapping with these complicated kinetic terms, a relatively simple kinetic term of the form  $\mathcal{H}_{kin} = -\Gamma(t) \sum_{<i,j>} (S_{<i,j>}^+ + H.C.)$  is used for the quantum to classical mapping. The Monte Carlo moves were kept restricted within the 2-opt family to avoid invalid tours. The results were tested on an instance of printed circuit board with  $N = 1002$ . PIMC-QA was seen to do better than the CA and also much better than standard Lin-Kernighan algorithm, as shown in Fig. 3. The relaxation behavior of residual path-length for TSP (see Fig. 3) is found to be quite similar to that of the 2-d EA glass discussed earlier (see Battaglia et al 2005). This indicates that a random TSP also has spin glass-like potential energy landscape (PEL), as has already been hinted by the replica analysis study of the problem dis-

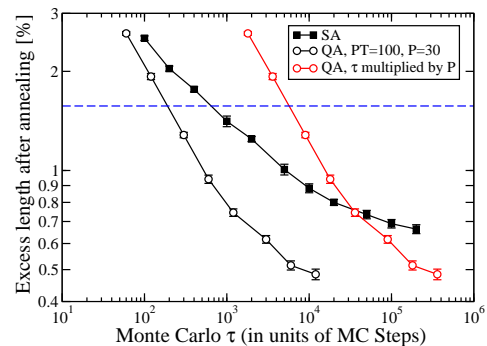


FIG. 3 Average residual excess length found after CA and QA for a total time  $\tau$  (in MC steps), for the  $N = 1002$  instance `pr1002` of the TSPLIB. The dashed horizontal line represents the best out of 1000 runs of the Lin-Kernighan algorithm. QA is clearly faster than CA (taken from Battaglia et al 2005).

cussed in an earlier section (Sec. IIC.2). In that case the Landau-Zener tunneling picture would also be applicable for TSP, and little improvement can be expected by following the real-time Schrödinger dynamics instead of Monte Carlo methods.

There are cases where PIMC-QA is not as successful as CA. An example (discussed below) of such a problem belongs to the class of  $K$ -Satisfiability problem (or  $K$ -SAT). In a  $K$ -SAT problem, there is a given Boolean function, which is the Boolean sum (connected by logical OR operations) of a number of clauses, each of which is a Boolean product (connected by logical AND operations) of  $K$  Boolean variables (binary variables taking values 0 or 1 only) taken random from a given set of  $p$  variables (same variable may occur in various clauses simultaneously). Given such a function, the task is to find an assignment for the Boolean variables for which the number of violated clauses [the clauses assigned with the 0 value] is the minimum. The studies on this class of problems is extensive and it even includes the connection between its hardness and satisfiability-unsatisfiability phase transition (Monasson et al 1999). Remarkable progress has been made in formulating faster algorithms for solving it (see Mezard et al 1987, Hartmann and Rieger 2002) based on these understandings.

But in the case of the random 3-SAT problem ( $K$ -SAT problem with  $K = 3$ ) using linear schedule for decreasing  $\Gamma$ , PIMC-QA gives much worse results than CA (Battaglia et al 2004). Both CA and PIMC-QA are worse than ad-hoc local search heuristics like WALKSAT. In the case of application of PIMC-QA in image restoration, on the other hand, the performance is exactly the same as that of CA (Inoue 2005). Even for a particle in a simple double-well potential, it seems that with naive Monte Carlo moves, PIMC-QA can produce results which are much worse than that one could obtain from real-time Schrödinger evolution of the system. There is in fact no general prescription to choose the right moves that will do the job, unless one has a precise idea about the PEL

of the problem. The choice of the kinetic term to be introduced into the problem is somewhat arbitrary but the performance of the algorithm depends on crucially on that. It has been found that a relativistic kinetic term can do a better job than a non-relativistic one in the case of a particle in a double-well potential (Battaglia et al 2005). PIMC-QA also suffers from difficulty in calculating the Suzuki-Trotter equivalent of the quantum Hamiltonian with arbitrary kinetic term designed to satisfy the constraints of the problem (Marton'ak et al, 2004). The constraints may be taken care of while making Monte Carlo moves, but that may not always produce expected results. Finally, presence of finite temperature in the problem does not allow one to focus exclusively on the role of the quantum fluctuations in the problem. Above all, like any other Monte Carlo method, PIMC-QA is going to do worse if the number of reasonably good approximate solutions are only few, and there is no overall gradient in the landscape to guide towards them.

### 3. Random Field Ising Model: How a Choice of Kinetic Term Improves Annealing Results

QA algorithms enjoy an extra flexibility which a thermal annealing algorithm cannot. A QA algorithm can have a host of choices for its kinetic term. A good choice can bring about a lot of betterments. This point is illustrated nicely by Morita and Nishimori (see Morita and Nishimori 2007a) for QA of random field Ising model, by introducing a ferro-magnetic transverse field interaction, in addition to the conventional single-spin-flip transverse field term (as present in the Hamiltonian (9)).

The Hamiltonian of the random-field Ising model with the standard single-spin-flip transverse term is given by

$$\mathcal{H}(t) = \mathcal{H}_C + \mathcal{H}_{Kin}^{(1)}, \quad (18)$$

where

$$\mathcal{H}_C = -J \sum_{\langle ij \rangle} S_i^z S_j^z - \sum_{i=1}^N h_i^z S_i^z, \quad (19)$$

$h_i^z$  being the on site random field assuming values +1 or -1 with equal probabilities and  $\langle ij \rangle$  denotes sum over the nearest neighbor on a 2-dimensional square lattice, and

$$\mathcal{H}_{Kin}^{(1)} = \Gamma(t) \sum_{i=1}^n S_i^x. \quad (20)$$

The result of QA in such a system is not satisfactory when  $J$  is much larger than  $h_i^z$  (Sarjala et al 2006). If a ferromagnetic transverse term of the form

$$\mathcal{H}_{kin}^{(2)} = -\Gamma(t) \sum_{\langle ij \rangle} S_i^x S_j^x \quad (21)$$

is added to the Hamiltonian (18), the result of QA is seen to improve considerably (Morita and Nishimori 2007a). This happens (as indicated by exact diagonalization results on small system) because the ferromagnetic transverse field term effectively increases the gap between the ground state and the first excited state and thus decreases the characteristic timescale for the system. This is an example of how one can utilize the flexibility in choosing the kinetic term in QA to formulate faster algorithms. This also indicates how the knowledge of the phase diagram of the system, the position of the quantum critical point in particular (where the gap tends to vanish), helps in choosing additional kinetic terms and thus allows for the annealing paths that can avoid, to some extent, the regions of very low gap.

### B. Quantum Annealing Using Real-time Adiabatic Evolution

QA is basically the analog version of quantum computation. Like the conventional analog quantum computation, the hardware realization of adiabatic quantum annealing is rather problem specific. But once realized, it follows the real-time Schrödinger evolution, whose exact simulation is always intractable (run time grows exponentially with the system size) for classical computers and often also even for digital quantum computers (see Nielsen and Chuang 2000). The annealing behavior with the real-time Schrödinger evolution is hence an important issue and may show features distinctly different from any Monte Carlo annealing discussed so far.

The first analog algorithm in this line was due to Farhi and Gutmann (1998) for solving Grover's search problem. Grover (1997) showed that quantum mechanical search can reduce an  $\mathcal{O}(N)$  classical search time to  $\mathcal{O}(\sqrt{N})$  time in finding out a marked item from an unstructured database. In the analog version, the problem was to use quantum evolution to find a given marked state among  $N$  orthonormal states. The algorithm was formulated in the following way. There were  $N$  mutually orthogonal normalized states, the  $i$ -th state being denoted by  $|i\rangle$ . Among all of them, only one, say, the  $w$ -th one, has energy  $E \neq 0$  and the rest all have zero energy. Thus the state  $|w\rangle$  is "marked" energetically and the system can distinguish it thus. Now the question is how fast the system can evolve under a certain Hamiltonian (our oracle) so that starting from an equal superposition of the  $N$  states one reaches  $|w\rangle$ . It was shown (Farhi and Gutmann 1998) that by evolving the system under a time-independent Hamiltonian of the form

$$\mathcal{H}_{tot} = E|w\rangle\langle w| + E|s\rangle\langle s|, \quad (22)$$

where

$$|s\rangle = \frac{1}{\sqrt{N}} \sum_{i=1}^N |i\rangle, \quad (23)$$

no improvement over Grover's  $\sqrt{N}$  speedup is possible. Later the problem was recast in the form of a spatial search (Childs and Goldstone 2004), where there is a  $d$ -dimensional lattice and the basis state  $|i\rangle$  is localized at the  $i$ -th lattice site. Similarly, as before, the on-site potential energy  $E$  is zero everywhere except at  $|w\rangle$ , where it is 1. The objective is to reach the marked state starting from the equal superposition of all the  $|i\rangle$ s. The kinetic term is formulated through the Laplacian of the lattice, which effectively introduces uniform hopping to all nearest neighbors from any given lattice site and is kept constant. The model is in essence an Anderson model (Santoro and Tosatti, 2006) with only a single-site disorder of strength  $\mathcal{O}(1)$ . Grover's speed up can be achieved for  $d \geq 4$  with such a Hamiltonian and no further betterment is possible. The algorithm succeeds only near the critical value of the kinetic term (i.e., at the quantum phase transition point). An adiabatic quantum evolution algorithm for Grover search was formulated in terms of an orthonormal complete set of  $l$ -bit Ising-like basis vectors, where the potential energy of a given basis vector (among the  $2^l$  ones) is 1, and for rest of all, it is 0. The kinetic term is just the sum of all single bit-flip terms (as the transverse-field term in Eq. (9)). It connects each basis vector to all those that can be reached from it by a single bit flip. The kinetic term is reduced from a high value to zero following a linear schedule. A detailed analysis in light of the adiabatic theorem showed that one cannot even retrieve Grover's speedup sticking to the global adiabatic condition with fixed evolution rate as given by Eq. (16). This is so because the minimum value of the gap goes as  $\Delta_{min} \sim 2.2^{-l/2}$  (Farhi et al 2000), and the spin-flip kinetic term being local, the numerator  $|\langle \mathcal{H}_{tot} \rangle|$  of the adiabatic factor (see Eq. (16)) is at best  $\mathcal{O}(l)$ . However, the Grover's speedup can be recovered if the condition of adiabaticity is maintained locally at every instant of the evolution and the rate is accelerated accordingly whenever possible (Roland and Cerf, 2001).

There is an equivalence between adiabatic quantum computation and the gate-based standard quantum computation (see Aharonov et al, 2004, Santoro and Tosatti 2007) in the sense that for any task that can be performed by a standard quantum circuit, there exists a time-dependent Hamiltonian  $\mathcal{H}(t)$  that does the same job evolving adiabatically.

Adiabatic QA following real-time Schrödinger evolution for satisfiability problems also gives strikingly different result (for smaller system-size, though) compared to that obtained using PIMC-QA. Adiabatic QA of an NP-complete problem, namely, the exact cover problem (as described below) is studied for small systems, where a quadratic system-size dependence was observed (Farhi et al 2001). In this problem also, the basis vectors are the complete set of  $2^l$  orthonormal  $l$ -bit basis vectors, denoted by  $\{|z_1\rangle \dots |z_l\rangle\}$ , each  $z_i$  is either 0 or 1. The problem consists of a cost function  $\mathcal{H}_C$  which is the sum of many 3-bit clause functions  $h_{Cl}(z_i, z_j, z_k)$ , each acting on arbitrarily chosen bits  $z_i, z_j$  and  $z_k$ . The clause

function is such that  $h_{Cl}(z_i, z_j, z_k) = 0$  if the clause  $Cl$  is satisfied by the states  $|z_i\rangle, |z_j\rangle$  and  $|z_k\rangle$  of the three bits, or else  $h_{Cl}(z_i, z_j, z_k) = 1$ . The cost Hamiltonian is given by  $\mathcal{H}_C = \sum_{Cl} h_{Cl}$ . Thus if a basis state  $|\{z_i\}\rangle$  dissatisfies  $p$  clauses, then  $\mathcal{H}_C|\{z_i\}\rangle = p|\{z_i\}\rangle$ . The question is whether there exists a basis vector that satisfies all the clauses for a given  $\mathcal{H}_C$ . There may be many basis vectors satisfying a clause. All of them will be the ground state of  $H_C$  with zero eigenvalue. If the ground state has a non-zero (must be a positive integer then) eigenvalue, then it represents the basis with lowest number of violated clauses, the number being given by the eigenvalue itself. The total Hamiltonian is given by

$$\mathcal{H}_{tot}(t) = \left(1 - \frac{t}{\tau}\right) \mathcal{H}_{kin} + \frac{t}{\tau} \mathcal{H}_C, \quad (24)$$

where  $\mathcal{H}_{kin}$  is again the sum of all the single bit-flip operators. The initial state at  $t = 0$  is taken to be the ground state of  $\mathcal{H}_{kin}$ , which is an equal superposition of all basis vectors. The system is then evolved according to the time-dependent Schrödinger equation up to  $t = \tau$ . The value of  $\tau$  required to achieve a pre-assigned success probability are noted for different system sizes. The result showed a smooth quadratic system size dependence for  $l \leq 20$  (Farhi et al 2001). The result is quite encouraging (since it seems to give a polynomial time solution for an NP-complete problem for small system size), but does not really assure a quadratic behavior in the asymptotic ( $l \rightarrow \infty$ ) limit.

A quadratic relaxation behavior ( $\epsilon_{res} \sim 1/\tau^\zeta$ ,  $\zeta \sim 2$ ) was also reported in (Suzuki and Okada 2005a, 2005b) for real-time adiabatic QA (employing exact method for small systems and DMRG technique for larger systems) of a one-dimensional tight-binding model with random site energies and also for a random field Ising model on 2-d square lattice. In the first case, the kinetic term was due to hopping between nearest neighbors, while in the second case it was simply the sum of single-spin flip operators as given in Eq. (9). Wave function annealing results using similar DMRG technique for spin glass on ladder has been reported by Rodriguez-Laguna (2007).

It has been demonstrated that for finite-ranged systems, where the interaction energy can be written as a sum of interaction energies involving few variables, quantum adiabatic annealing and thermal annealing may not differ much in efficiency. However, for problems with spiky (very high but narrow) barriers in the PEL (which must include infinite-range terms in the Hamiltonian, since in finite-range systems, barrier heights can grow at best linearly with barrier width), quantum annealing does much better than CA (Farhi and Goldstone 2002) as has been argued by Ray et al (Ray et al 1989). Quantum adiabatic evolution has been employed earlier to study the SK spin glass in a transverse field; stationary characteristics over a range of the transverse field are calculated by varying the transverse field adiabatically (Lancaster and Ritort 1997).

As pointed out earlier in the case of PIMC-QA, the

kinetic term plays a crucial role in adiabatic QA also. This is mainly because the gap  $\Delta(\Gamma)$  between the ground state and first excited state depends on the form of  $\mathcal{H}_{kin}$ . For certain choice of  $\mathcal{H}_{kin}$ , it might become very small for some  $\Gamma$ . One then can switch on some additional kinetic term (adjusted by another parameter  $\Gamma'$ ) to increase the dimensionality of the phase diagram and avoid the small gap zone by taking a suitable by-pass. In fact such a strategy can convert a failure into success (Farhi et al 2002).

So far it has been argued that the advantage of quantum annealing derives mainly from the fact that quantum tunneling can penetrate through very high but narrow barriers, which are very hard to jump over thermally. In this way the cost-configuration landscapes more accessible to local moves. This is a key feature that works even in the case of quantum Monte Carlo methods like PIMC-QA, where one finally samples only a very small section of the configuration space. However, another remarkable advantage that quantum mechanics provides is the ability to “sense” the whole configuration space simultaneously through a delocalized wave function. This sensing is largely handicapped by presence of random disorder in the system, because the wave function tends to localize in many places, often being unable to pick up the deepest well very distinctly. But this feature may be utilized in searching a golf-course-like PEL, namely a flat landscape with very deep and narrow wells occurring very rarely. If there is only one deep well, the problem is just the spatial version of the Grover’s problem. As we have seen, if the depth  $\chi$  of the well is  $\mathcal{O}(1)$  (independent of  $N$ ), then no more than  $\mathcal{O}(\sqrt{N})$  speed-up can be achieved. This can be interpreted as the inability of an exceedingly large system to sense a given small wound. So one might want to make the depth of the well large enough so that it cannot be scaled away as the system-size is increased.

We first consider the case where the well-depth goes as  $\chi \sim \alpha N$ , where  $\alpha$  is some constant. For a well depth of such order for a spatial search at infinite dimension (kinetic term is infinite-ranged) one gets a stunning result: The evolution time that guarantees any given probability of success becomes independent of  $N$  (Das 2007; see Fig. 4). However, if  $\chi$  scales like  $\chi \sim N^\gamma$ , with  $\gamma > 1$ , then the speed-up is lost again - a consequence of quantum-mechanical non-adiabaticity. We formulate the problem in the following way. As in the case of a spatial search discussed above, we denote the state localized at the  $i$ -th cite by  $|i\rangle$ . All the cites except  $|w\rangle$  has zero on-site potential energy, while  $|w\rangle$  have an on-site potential well of depth  $\chi(t)$ . The system is embedded in infinite dimensions and thus there is a uniform tunneling term  $\Gamma$  between any two sites. To do quantum annealing, we evolve  $\chi(t)$  from zero to its final value  $\chi_0$  keeping  $\Gamma$  fixed at some moderate constant value. The total Hamiltonian is given by

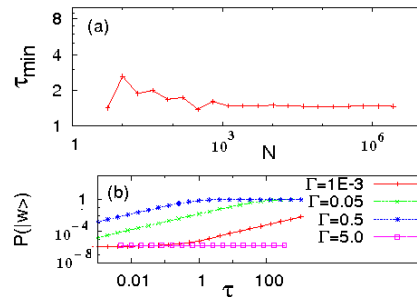


FIG. 4 Panel (a) in the figure shows numerical verification of the  $N$ -independence of the minimum time  $\tau_{min}$  to achieve success probability  $P(|w\rangle) = 0.33$ . Initially, the system is delocalized equally over all sites and evolves with time according to time dependent Schrödinger equation with the Hamiltonian (25). As expected from exact analytical result for the adiabaticity condition, it is seen that  $\tau_{min}$  becomes independent of  $N$ . Panel (b) shows the variation of final probability  $P(|w\rangle)$  of finding the state  $|w\rangle$  with annealing time  $\tau$  for different final value of  $\Gamma$ , for  $N = 10^6$ .

$$\mathcal{H}_{tot} = -\chi_0 (1 - t/\tau) |w\rangle\langle w| - \Gamma \sum_{i,j;i \neq j} |i\rangle\langle j|. \quad (25)$$

The time-dependent eigen problem can be solved for the above Hamiltonian. It can be shown exactly that if  $\chi_0 \sim \alpha N$ , then in the  $N \rightarrow \infty$  limit, the adiabatic factor

$$\frac{|\langle \dot{\mathcal{H}}_{tot} \rangle|_{max}}{\Delta_{min}^2(t)} \sim \frac{\alpha}{4\Gamma^2}, \quad (26)$$

which means that the run time becomes independent of  $N$ , and the ground state has  $\mathcal{O}(1)$  overlap with the target state  $|w\rangle$ . We also confirm it numerically by evaluating  $\tau_{min}$ , which is the minimal  $\tau$  required for obtaining a success probability  $P(|w\rangle) = 0.33$  for different  $N$  through many decades. Here we have chosen a moderate constant  $\Gamma$ , and have evolved the well depth  $\chi$  with time. The evolution is computed by solving the time-dependent Schrödinger equation numerically and  $\tau_{min}$  is obtained with an accuracy of  $10^{-4}$  by employing a bisection scheme. The results (Fig. 4a) clearly show that  $P(|w\rangle)$  tends to become independent of  $N$  as  $N$  becomes larger and larger. This is completely in accordance with the analytical result (see Eq. (26)).

The relaxation behavior for large  $N$  for a given annealing time  $\tau$  depends on the value of  $\Gamma$  (see Fig. 4b). If  $\Gamma$  is too small, the system takes a longer time to feel the changes in the landscape, and hence the adiabatic relaxation requires a longer time (the adiabatic factor becomes bigger; see Eq. (26)). On the other hand, if  $\Gamma$  is too large, the ground state itself is pretty delocalized, and hence the final state, though closer to the ground state, has again a small overlap with the target state  $|w\rangle$ . For  $\Gamma = 0.5$ , the result is best. For higher and lower values of  $\Gamma$ , the results are worse, as shown in Fig. 4(b). The relaxation behavior is seen to be linear with the annealing time  $\tau$ .



### C. Annealing of a Kinetically Constrained System

The adiabatic theorem of quantum annealing assures convergence of a quantum algorithm when one starts with the initial (trivial) ground state of the Hamiltonian and evolves slowly enough so that the system is always in the ground state of the instantaneous Hamiltonian. However, the benefit of tunneling may be extended even in cases where one does not precisely know the eigenstate of the initial Hamiltonian (say for a given unknown PEL) and hence is unable to start with it. One might rather start with a wave-packet (a superposition of many eigenstates of the Hamiltonian) that explores the potential energy landscape. Quantum tunneling will still allow it to move more easily through the PEL than a classical particle if the landscape has many high but narrow barriers. A semi-classical treatment of such a non-stationary annealing has been discussed in the context of a kinetically constrained system (KCS) (Das et al 2005).

We demonstrate here the effectiveness of quantum annealing in the context of a certain generalized Kinetically Constrained Systems (KCS) (Fredrickson and Andersen et al 1984). KCSs are simple model systems having trivial ground state structures and static properties, but a complex relaxation behavior due to some explicit constraints introduced in the dynamics of the system. These systems are very important in understanding how much of the slow and complex relaxation behavior of a glass can be attributed to its constrained dynamics alone, leaving aside any complexity of its energy landscape structure. In KCSs one can view the constraints to be represented by infinitely high energy barriers appearing dynamically.

We discuss quantum annealing in the context of a KCS, which can be represented by a generalized version of the East model (Jackle and Eisinger 1991); a one dimensional KCS. We also compare the results with that of thermal annealing done in the same system. The original East model is basically a one-dimensional chain of non-interacting classical Ising ('up-down') spins in a longitudinal field  $h$ , say, in downward direction. The ground state of such a system is, trivially, all spins down. A kinetic constraint is introduced in the model by putting the restriction that the  $i$ -th spin cannot flip if the  $(i-1)$ -th spin is down. Such a kinetic constraint essentially changes the topology of the configuration space, since the shortest path between any two configurations differing by one or more forbidden flips is increased in a complicated manner owing to the blockage of the 'straight' path consisting of direct flips of the dissimilar spins. Further, the constraint becomes more limiting as more spins turn down, as happens in the late approach to equilibrium. As a result, the relaxation processes have to follow more complex and lengthier paths, giving rise to exponentially large timescale ( $\sim e^{1/T^2}$ ; Jackle and Eisinger 1991).

In the Das model (Das et al 2005) there is a chain of asymmetric double-wells (each with infinite boundary walls), each having a particle localized within them. The asymmetry is due to an energy difference of  $2h$  between

the two wells of a double well. The particle in one of the two (asymmetric) wells can change its location to the other well stochastically, either due to the thermal fluctuations or the quantum fluctuations present in the system. The generalized kinetic constraint is introduced by assuming that if the particle in the  $(i-1)$ -th double-well resides in the lower one of the two wells, then there appears a barrier of height  $\chi$  and width  $a$  between the two wells of the  $i$ -th double-well. In such a situation the particle in the  $i$ -th double-well has to cross the barrier in order to change its location from one well to the other. On the other hand, if the particle of the  $(i-1)$ -th is in its upper well, there is no such barrier to cross for the particle to go from one well to the other. Following the approximate mapping done in case of a symmetric double-well (Chakrabarti et al 1996), this model can be approximately represented by a generalized version of the East model, where each Ising spin is in a local longitudinal field  $h$  in the downward direction. The spin at the  $i$ -th site sees a barrier of height  $\chi$  and width  $a$  between its two energy states when the  $(i-1)$ -th spin is down, while no such barrier occurs for the  $i$ -th spin when the  $(i-1)$ -th spin is up. This kinetic constraint is the same in both cases irrespective of whether the dynamics is classical or quantum.

When the dynamics of the particle is due to quantum fluctuations, the tunneling probabilities come from the following semi-classical picture of scattering of a particle in a double-well with infinitely remote outer boundaries. If a particle is put in one of the wells of such a double-well with some kinetic energy (actually the expectation value)  $\Gamma$ , then it will eventually be scattered by the separator (a barrier or step) between the two wells. In such a scattering, there is a finite probability  $P$  that the particle manages to go to the other well. We calculate  $P$  from the simple picture of scatterings of a particle by one dimensional potentials as described below. In the thermal case we take simple Boltzmann probabilities for crossing the same barriers. The minimum of the energy of the Ising chain (equivalent to the potential energy of the chain of the double-wells) trivially corresponds to the state with all the spins down, i.e., aligned along the longitudinal field  $h$  (where all the particles are in their respective lower wells). To reach the ground state in the quantum case, we start with a very large initial value of  $\Gamma$  and then reduce it following an exponential schedule given by  $\Gamma = \Gamma_0 \exp(-t/\tau_Q)$ . Here  $t$  denotes the time and  $\tau_Q$  sets the effective time scale of annealing. At zero-temperature the slow spin flip dynamics occurs only due to the tunneling (kinetic energy) term  $\Gamma$  and hence the system ceases to have any relaxation dynamics in the limit  $\Gamma \rightarrow 0$ . The barriers are characterized by a height  $\chi$  and a width  $a$ , the barrier area being  $g = \chi \times a$ . Similarly, in thermal case, we start with a high initial temperature  $T_0$  and reduce it eventually following an exponentially decreasing temperature schedule given by  $T = T_0 \exp(-t/\tau_C)$ ;  $\tau_C$  being the time constant for the thermal annealing schedule. Here, when the  $(i-1)$ -th spin is down, the flipping



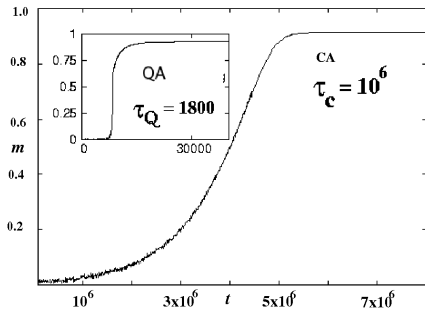


FIG. 5 Comparison between classical and quantum annealing for a chain of  $5 \times 10^4$  spins (for the same initial disordered configuration with  $m_i \sim 10^{-3}$ ). We show the results for  $\tau_Q = 1.8 \times 10^2$  (for quantum) and  $\tau_C = 10^6$  (for classical) with  $h = 1$ ; a lower  $\tau_C$  would not produce substantial annealing. Starting from the same initial values  $\Gamma_0 = T_0 = 100$ , (and  $g = 100$  in the quantum case) we observe that classical annealing requires about  $10^7$  steps, whereas quantum annealing takes about  $10^4$  steps for achieving the same final order  $m_f \sim 0.92$ .

probability for the  $i$ -th spin ( $\sim \exp(-\chi/T)$ ). Otherwise, it flips with probability  $P = 1$  if it were in the up state and with Boltzmann probability  $P = \exp(-h/T)$  if it were in the down state. Here in the quantum case, the probability of crossing the barrier depends on  $g$  so that the barrier-width  $a$  plays a role, while in the thermal case, only  $\chi$  sets the crossing timescale irrespective of  $a$ .

In the simulation (Das et al 2005),  $N$  Ising spins ( $S_i = \pm 1$ ,  $i = 1, \dots, N$ ) were taken on a linear chain with periodic boundary condition. The initial spin configuration is taken to be random, so that the magnetization  $m = (1/N) \sum_i S_i$  is practically negligible ( $m_i \approx 0$ ). We then start with a tunneling field  $\Gamma_0$  and follow the zero-temperature (semi-classical) Monte Carlo scheme as mentioned above, using the spin flip probabilities  $P$ 's appropriate for the four cases I-IV. Each complete run over the entire lattice is taken as one time unit and as time progresses,  $\Gamma$  is decreased from its initial value  $\Gamma_0$  according to  $\Gamma = \Gamma_0 e^{-t/\tau_Q}$ . The results of thermal and quantum annealing are compared in Fig. 5 for the same order of initial value and time constant for  $\Gamma$  and  $T$  (the barrier height  $\chi$  is taken to be 1000 in both the cases, and  $g$  was taken to be 100 in the quantum annealing case, or equivalently the barrier width  $a$  is taken to be of the order of 0.1). It is observed that to achieve a similar degree of annealing (attaining a certain final magnetization  $m_f$ ), starting from the same disordered configuration, one typically requires much smaller  $\tau_Q$  compared to  $\tau_C$ ; typically,  $\tau_C \sim 10^3 \times \tau_Q$  for equivalent annealing (for similar optimal values of final order  $m_f \sim 0.92$ ). For annealing with final order  $m_f \sim 1$ , we find  $\tau_C \sim 10^4 \times \tau_Q$ . This comparison depends on the barrier characteristics (the value of  $g$ ).

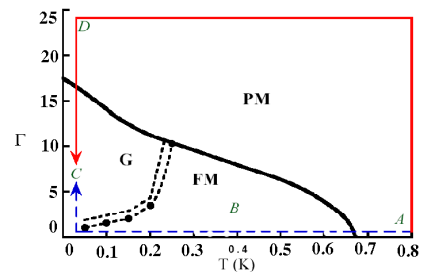


FIG. 6 Experimental realization of QA and CA in  $\text{LiHo}_{0.44}\text{Y}_{0.56}\text{F}_4$  is illustrated on its phase diagram on the temperature  $T$  and transverse field  $\Gamma$  (measured by the magnitude of the external laboratory field in kOe) plane. The material behaves like a conventional ferromagnet in the region labeled FM, and shows slow relaxation in the glassy domain wall state labeled G. The two paths of relaxations, from an initial point A to a final point C on the phase diagram are shown by arrow-headed lines. Along the classical path  $A \rightarrow B \rightarrow C$  (dashed arrow) the transverse field is not applied until the end, so that the relaxations observed are purely thermal. Whereas, along the quantum path  $A \rightarrow D \rightarrow C$  (continuous arrow), there is a segment where the temperature is small enough and the transverse field is high, so that the fluctuations are mainly quantum mechanical. Relaxations observed along the quantum path are often found to be much faster than those observed along the classical path at low enough temperature. Taken from Aeppli and Rosenbaum (2005).

#### D. Experimental Realization of Quantum Annealing

Brook et al (1999) showed experimentally (see also Aeppli and Rosenbaum 2005) that the relaxation behavior in reaching deep inside the glass phase in Fig. 6 depends on the path chosen.

A TISG, realized by a sample of  $\text{LiHo}_{0.44}\text{Y}_{0.56}\text{F}_4$  in laboratory transverse field ( $\Gamma$ ), was taken from a high temperature paramagnetic to a low temperature glassy phase following two separate paths in the  $\Gamma - T$  plane (see Fig. 6). Along the classical path of cooling (CA), the transverse field was kept zero throughout, and was switched on only after reaching the final temperature. The quantum cooling (QA), on the other hand, was done in the presence of a high transverse field, which was lowered only on reaching the final temperature. As the sample is cooled, spectroscopy of the sample at different temperatures (both during CA and QA) was done to reveal the nature of the distribution of spin relaxation time scales. The QA produced states whose relaxation was up to 30 times faster than those produced by the CA at low temperature (see Aeppli and Rosenbaum 2005). This clearly indicates that quantum tunneling is much more effective in exploring the configuration space in the glassy phase than thermal jumps (as indicated in Fig. 1).

An experimental realization of quantum adiabatic annealing for 3-bit instances of MAXCUT problem using NMR technique has also been reported (see Steffen et al 2003). Here, the smoothly varying time dependent Hamiltonian was realized by the technique of quan-

tum simulation (see Nielsen and Chuang 2000), where a smooth time evolution was achieved approximately (Trotter approximation) through the application of a series of discrete unitary operations. The results indicate existence of an optimal run time of the algorithm.

#### IV. CONVERGENCE OF QUANTUM ANNEALING ALGORITHMS

Here we briefly summarize some important recent results derived by Morita and Nishimori (2006, 2007b) on the convergence of QA algorithms for TIM systems. The results are valid for both the Quantum Monte Carlo and the real-time Schrödinger evolution versions of QA.

The Hamiltonian here is the same as given in (9) with a time dependence in the transverse field  $\Gamma = \Gamma(t)$ . No assumption regarding either the nature of the distribution of  $J_{ij}$  or the spatial dimensionality is required. In order to perform QA at temperature  $T$  using PIMC, one constructs the Suzuki-Trotter equivalent (see Appendix 1)  $d+1$  dimensional classical system of the  $d$  dimensional quantum system, and the resulting (classical) system is simulated using a suitable inhomogeneous Markov Chain. The transverse field  $\Gamma(t)$  is tuned from a high value to zero in course of simulation. It can be shown that at the end of the simulation the final distribution converges to the ground state of the classical part of the Hamiltonian irrespective of the initial distribution (strong ergodicity) if

$$\Gamma(t) \geq MT \tanh^{-1} \left[ \frac{1}{(t+2)^{2/RL}} \right], \quad (27)$$

where  $M$  is the number of Trotter replicas in the  $d+1$  dimensional Suzuki-Trotter equivalent system. Here  $R$  and  $L$  are constants depending on the system size  $N$ , the spin-flip dynamics appointed for the simulation, the temperature  $T$ , etc. For large  $t$  the bound reduces to

$$\Gamma(t) \geq MT \frac{1}{(t+2)^{2/RL}}. \quad (28)$$

It is remarkable that in contrast to the inverse logarithmic decay of temperature required for convergence of CA (see Eq. 1), QA requires only a power-law decay of the transverse field. In this sense, quantum annealing is much faster than the classical annealing for TIM. Similar result can be derived for more general form of Hamiltonian (see Morita and Nishimori 2006). However, the advantage gained here does not change the complexity class of an NP-complete problem, since  $RL$  is of the order of  $N$  and hence the convergence time is thus still exponential in  $N$ .

For real-time Schrödinger dynamics at  $T = 0$ , the bound for the decay of the transverse field is again of the form

$$\Gamma(t) \geq (\xi t)^{-\frac{1}{(2N-1)}}, \quad (29)$$

where  $\xi$  is exponentially small in  $N$  for large  $N$ . Though the dynamics of PIMC-QA and real-time Schrödinger evolution are completely different, the power-law bound on the annealing schedule is strikingly similar.

#### V. QUANTUM QUENCHING

Instead of annealing, one can quench a systems by reducing the transverse field from  $\Gamma_i (> \Gamma_c)$  to  $\Gamma_f (< \Gamma_c)$  and follow the relaxation dynamics after that. Here  $\Gamma_c$  denotes the quantum critical point for the system. This can help to prepare a state of the system with substantial order in a very short time. Recently, quantum quenching dynamics in different systems, in particular for sudden quenching across a quantum critical point, have been studied extensively (Sengupta et al 2005, Calabrese and Cardy 2006, Das et al 2006). The (exact) results for the after-quench dynamics, following a sudden quench of an infinite-range Ising model in transverse field (Das et al 2006, see Appendix 2) is shown in Fig. 7. The results indicate that for a purely quantum system (small  $S$ ), one might reach a non-stationary oscillatory state with a substantial value for the long-time average (over the largest timescale) of the order  $\langle (\sum S_i^z)^2(t) \rangle$  if the quenching is done from  $\Gamma_i > \Gamma_c$  to  $\Gamma_f = \Gamma_c/2$ . Thus one gets a state (though non-stationary) which has considerable order, in just one step quenching.

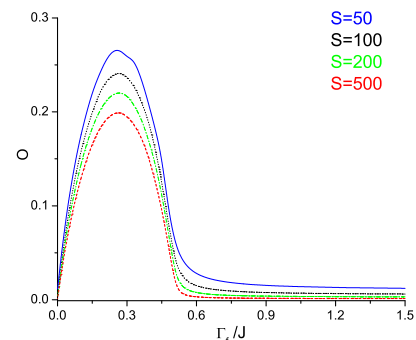


FIG. 7 Plot of the long-time average (see Appendix 2)  $O = \langle (S_{tot}^z)^2 \rangle$  as a function of  $\Gamma_f/J$  for different  $S$ . In the plot the solid (blue), dotted (black), dash-dotted (green) and the dashed (red) lines represents respectively the results for  $S = 50$ ,  $S = 100$ ,  $S = 200$  and  $S = 500$  (color online).  $O$  peaks around  $\Gamma_f/J = 0.25$  and the peak value decreases with increasing  $S$ . For all plots we have chosen  $\Gamma_i/J = 2$ . (The figure is taken from Das et al 2006).

#### VI. SUMMARY AND DISCUSSIONS

Unlike the gate-based quantum computers (see, e.g., Ekert and Jozsa 1996, Nielsen and Chuang 2000, Galindo and Martin-Delgado 2002), the annealing of a physical system towards the optimal state (encoded in the ground

state of the final Hamiltonian) in the classical limit naturally achieves analog quantum computation. As discussed here, the utilization of the quantum mechanical tunneling through the classically localized states in annealing of glasses has opened up this new paradigm for analog quantum computation of hard optimization problems through adiabatic reduction of the quantum fluctuations.

We reviewed here the recent success in annealing, or optimizing the cost functions of complex systems, utilizing quantum fluctuations rather than the thermal fluctuations (see Santoro and Tosatti 2006 for a more technical review). As mentioned already, following the early indication in Ray et al (1989) and the pioneering demonstrations, theoretically by Amara et al (1993), Finnila et al (1994), Kadowaki and Nishimori (1998), Farhi et al (2001) and Santoro et al (2002), and experimentally by Brook et al (1999), the quantum annealing technique has now emerged as a successful technique for optimization of complex cost functions. The literature, exploring its success and also its limitations, is also considerably developed at present.

These are introduced here through discussions of the mapping of such hard problems to classical spin glass problems, discussions on quantum spin glasses, and consequent annealing. The physics of classical spin glasses (see Sec. II) offers us the knowledge of the of the energy or the thermodynamic potentials and their landscape structures. Mapping of computationally hard problems like the traveling salesman etc problems to their corresponding classical spin glass models also helped understanding their complexity (Sec. IIC). The timescale for tunneling through an energy barrier quantum mechanically involves not only the height of the barrier, but also its width; the narrower the barrier, the faster the tunneling (the height being kept constant). Thermal fluctuations, on the other hand, see only the barrier height for crossing it. Thus, the reduction of tunneling time with the barrier width, an aspect which leads to faster relaxation due to quantum fluctuations than that due to the classical one in the context of spin glasses, leads to quantum annealing. This is a framework for constructing general heuristics to find approximate solutions of hard optimization problems. While simulated annealing employs the strategy of slow cooling, physical or in simulations, to find the ground state of glassy systems, quantum annealing employs quantum fluctuations (see Sec. III). As mentioned before, this effectively reduces Planck's constant to zero to reach the classically optimized (minimum cost) state. This reduction, when done completely adiabatically, guarantees that the system will be found in the ground state of the classical glass at the end (provided there is no crossing of energy levels with the ground state in the course of evolution, and one has started initially with the ground state of the Hamiltonian). This has already been realized experimentally (see Sec. IIID), where faster relaxation towards the ground state is achieved by reducing the external field (inducing

changes in the tunneling field), rather than by reducing the temperature. In this way analog quantum computation is realized through a novel route.

## Acknowledgments

We are grateful to A. Chakrabarti, P. Ray, D. Sen, K. Sengupta and R. B. Stinchcombe for their collaborations at different stages of this work. We acknowledge G. Aeppli, A. Dutta, H. Nishimori, G. Santoro, P. Sen and E. Tosatti for useful discussions.

## VII. APPENDIX

### 1. Suzuki-Trotter Formalism

Here we illustrate this formalism by applying it to a TIM having a Hamiltonian

$$\mathcal{H} = -\Gamma \sum_{i=1}^N S_i^x - \sum_{(i,j)} J_{ij} S_i^z S_j^z \equiv \mathcal{H}_{kin} + \mathcal{H}_C. \quad (30)$$

The canonical partition function of  $\mathcal{H}$  reads

$$Z = \text{Tr} e^{-(\mathcal{H}_{kin} + \mathcal{H}_C)/T}. \quad (31)$$

Now we apply the Trotter formula

$$\exp(A_1 + A_2) = \lim_{M \rightarrow \infty} [\exp A_1/M \exp A_2/M]^M, \quad (32)$$

even when  $[A_1, A_2] \neq 0$ . On application of this,  $Z$  reads

$$Z = \lim_{M \rightarrow \infty} \sum_i \langle s_i | [\exp(-\mathcal{H}_{kin}/MT) \times \exp(-\mathcal{H}_C/MT)]^M | s_i \rangle. \quad (33)$$

Here  $s_i$  represent the  $i$ -th spin configuration of the whole system, and the above summation runs over all such possible configurations denoted by  $i$ . Now we introduce  $M$  number of identity operators in between the product of  $M$  exponentials in  $Z$ , and have

$$Z = \lim_{M \rightarrow \infty} \text{Tr} \prod_{k=1}^M \langle S_{1,k} \dots S_{N,k} | \exp\left(\frac{-\mathcal{H}_{kin}}{MT}\right) \times \exp\left(\frac{-\mathcal{H}_C}{MT}\right) | S_{1,k+1} \dots S_{N,k+1} \rangle,$$

and periodic boundary condition would imply  $S_{N+1,p} = S_{1,p}$ . Now,

$$\begin{aligned} & \prod_{k=1}^M \langle S_{1,k} \dots S_{N,k} | \exp\left(\frac{1}{MT} \sum_{i,j} J_{ij} S_i^z S_j^z\right) | S_{1,k+1} \dots S_{N,k+1} \rangle \\ &= \exp \left[ \sum_{i,j=1}^N \sum_{k=1}^M \frac{J_{ij}}{MT} S_{i,k} S_{j,k} \right], \end{aligned}$$

where  $S_{i,k} = \pm 1$  are the eigenvalues of  $S^z$  operator (see Hatano and Suzuki, 2005), and

$$\begin{aligned} & \prod_{k=1}^M \langle S_{1,k} \dots S_{N,k} | \exp \left[ \frac{\Gamma}{MT} \sum_i S_i^x \right] | S_{1,k+1} \dots S_{N,k+1} \rangle \\ &= \left( \frac{1}{2} \sinh \left[ \frac{2\Gamma}{MT} \right] \right)^{\frac{NM}{2}} \times \\ & \exp \left[ \frac{1}{2} \ln \coth \left( \frac{\Gamma}{MT} \right) \sum_{i=1}^N \sum_{k=1}^M S_{i,k} S_{i,k+1} \right], \end{aligned}$$

giving the effective classical Hamiltonian (14), equivalent to the quantum one in (30).

It may be noted from above equation that  $M$  should be at the order of  $1/T$  ( $\hbar = 1$ ) for a meaningful comparison of the interaction in the Trotter direction with that in the original Hamiltonian. For  $T \rightarrow 0$ ,  $M \rightarrow \infty$ , and the Hamiltonian represents a system of spins in a  $(d+1)$ -dimensional lattice, because of the appearance of one extra label  $k$  for each spin variable. Thus corresponding to each single quantum spin variable  $S_i$  in the original Hamiltonian we have an array of  $M$  number of classical replica spins  $S_{ik}$ . This new (time-like) dimension along which these classical spins are spaced is known as Trotter dimension.

## 2. Quantum Quenching of a Long Range TIM

Let us consider a system of spin- $\frac{1}{2}$  objects governed by the Hamiltonian

$$\mathcal{H} = -\frac{J}{N} \sum_{i>j}^N S_i^z S_j^z - \Gamma \sum_i^N S_i^x. \quad (34)$$

It can easily be rewritten as

$$\mathcal{H} = -\frac{J}{N} (S_{tot}^z)^2 - \Gamma S_{tot}^x, \quad (35)$$

where  $S_{tot}^z = \sum_i S_i^z$ ,  $S_{tot}^x = \sum_i S_i^x$  and a constant  $(J/2N) \sum_i (S_i^z)^2 = J/8$  from  $\mathcal{H}$  in (35). The above Hamiltonian can again be cast into the simplified form

$$\mathcal{H} = \vec{h} \cdot \vec{S}_{tot}, \quad (36)$$

where  $\vec{h} = Jm\hat{z} - \Gamma\hat{x}$ , giving the mean field (exact in this long-range limit) equation

$$m \equiv \langle S_{tot}^z \rangle = \frac{|\vec{h} \cdot \hat{z}|}{|\vec{h}|} \tanh \left( \frac{|\vec{h}|}{T} \right) = \frac{Jm}{2\sqrt{\Gamma^2 + J^2 m^2}}, \quad (37)$$

at  $T = 0$  and  $\hat{z}$ ,  $\hat{x}$  denote unit vectors along  $z$  and  $x$  directions respectively. This gives  $m = 0$  for  $\Gamma > \Gamma_c$  and  $m \neq 0$  for  $\Gamma < \Gamma_c = J/2$ . Since the model is infinite-ranged one, the mean field approximation becomes exact

and one can readily express  $\vec{S}$  in terms of its polar components as  $\vec{S} = S(\sin \theta \cos \phi, \sin \theta \sin \phi, \cos \theta)$ ,  $S$  being the total angular momentum. One can immediately utilize the classical equation of motion  $\frac{d\vec{S}}{dt} = \vec{S} \times \vec{h}$ . Considering the above equation for the  $z$  and  $x$  components, we get

$$\frac{d\theta}{dt} = \Gamma \sin \theta \quad \text{and} \quad \frac{d\phi}{dt} = -\frac{J}{2} \cos \theta + \Gamma \cot \theta \cos \phi. \quad (38)$$

Here we have  $S = N/2$ . If the system is now quenched from above its quantum critical point  $\Gamma > \Gamma_c$ , finally to a  $\Gamma_f < \Gamma_c$ , then one can write (see Das et al 2006), equating the energies of the states with and without any order respectively,

$$\Gamma_f = \frac{J}{4} \cos^2 \theta + \Gamma_f \sin \theta \cos \phi. \quad (39)$$

Using this, one gets from Eq. (38)

$$\frac{d\theta}{dt} = \frac{\sqrt{\Gamma_f^2 \sin^2 \theta - [\Gamma_f - J/4 \cos^2 \theta]^2}}{\sin \theta} \equiv f(\theta). \quad (40)$$

This has zeros (turning points) at  $\theta_1 = \sin^{-1}(|1 - 4\Gamma_f/J|)$  and  $\theta_2 = \pi/2$ . One can therefore obtain  $\langle (S_{tot}^z)^2 \rangle = \langle \cos^2 \theta \rangle = \mathcal{N}/\mathcal{D}$ , where  $\mathcal{N} = \int_{\theta_1}^{\theta_2} d\theta \cos^2 \theta / f(\theta) = 4\sqrt{8\Gamma_f(J - 2\Gamma_f)/J}$  and  $\mathcal{D} = \int_{\theta_1}^{\theta_2} d\theta / f(\theta)$ , giving a behavior shown in Fig. 7.

## References

- [1] Aeppli G. and Rosenbaum T. F. (2005), in Das and Chakrabarti (2005), pp 159-169
- [2] Aharonov D., van Dam W., Kempe J., Landau Z., Lloyd S. and Regev O. (2004) arXiv:quant-ph/0405098
- [3] Alvarez J. A. and Ritort F. (1996), J. Phys. A **29**, 7355
- [4] Amara P., Hsu D., and Straub J. E. (1993), J. Phys. Chem. **97** 6715
- [5] Barahona F. (1982), J. Phys. A **15** 3241
- [6] Battaglia D. A., Santoro G. E. and Tosatti E. (2004), Phys. Rev. E **70** 066707
- [7] Battaglia D. A., Stella L., Zagordi O., Santoro G. E. and Tosatti E. (2005), in Das and Chakrabarti (2005), pp 171-204
- [8] Bearwood J., Halton J. H., Hammersley J. H. (1959), Proc. Camb. Phil. Soc. **55** 299
- [9] Bhatt R. N. (1998), in *Spin Glasses and Random Fields*, Young A. P. (Ed.), World Scientific, Singapore, pp. 225 - 249
- [10] Binder K. and Young A. P. (1986), Rev. Mod. Phys. **58** 801
- [11] Bray A. J. and Moore M. A. (1984), J. Phys. C Lett. **17** L463
- [12] Brook J., Bitko D., Rosenbaum T. F. and Aeppli G. (1999), Science **284** 779
- [13] Calabrese P. and Cardy J. (2006), Phys. Rev. Letts. **96** 136801
- [14] Chakrabarti B. K. (1981), Phys. Rev. B **24** 4062

- [15] Chakrabarti B. K., Dutta A. and Sen P. (1996), *Quantum Ising Phases and Transitions in Transverse Ising Models*, Springer-Verlag, Heidelberg
- [16] Chakraborti A. and Chakrabarti B. K. (2000), Euro. Phys. J. B **16** 667
- [17] Childs A. M. and Goldstone J. (2004), arXiv:quant-ph/0306054
- [18] Das A. (2007), In preparation
- [19] Das A. and Chakrabarti B. K. (2005) Eds., *Quantum Annealing and Related Optimization Methods*, Lecture Note in Physics, **679**, Springer-Verlag, Heidelberg
- [20] Das A., Chakrabarti B. K. and Stinchcombe R. B. (2005), Phys. Rev. E **72** 026701
- [21] Das A., Sengupta K., Sen D., Chakrabarti B. K. (2006), Phys. Rev. B **74** 144423
- [22] Dotsenko V. (2001) *Introduction to the Replica Theory of Disordered Statistical Systems*, Cambridge University Press, Cambridge, UK
- [23] Edwards S. F. and Anderson P. W. (1975), J. Phys. F: Met. Phys. **5** 965
- [24] Ekert A. and Jozsa R. (1996), Rev. Mod. Phys. **68** 733
- [25] Farhi E. and Gutmann S. (1998), Phys. Rev. A **57** 2403
- [26] Farhi E., Goldstone J., Gutmann S. and Sipser M. (2000) Preprint quant-ph/0001106
- [27] Farhi E., Goldstone J., Gutmann S., Lapan J., Ludgren A. and Preda D. (2001), Science **292** 472
- [28] Farhi E. and Goldstone J. (2002), arXiv:quant-ph/0201031
- [29] Farhi E., Goldstone J. and Guttmann S. (2001), arXiv:quant-ph/0208135
- [30] Finnila A. B., Gomez M. A., Sebenik C., Stenson C., and Doll D. J. (1994), Chem. Phys. Lett. **219**, 343
- [31] Fisher D. S. and Huse D. A. (1986), Phys. Rev. Lett. **56**, 1601
- [32] Fredrickson G. H. and Andersen H. C. (1984), Phys. Rev. Lett. **53** 1224
- [33] Fu Y. and Anderson P. W. (1986), J. Phys. A **19** 1620
- [34] Galindo A. and Martin-Delgado M. A. (2002), Rev. Mod. Phys. **74** 347
- [35] Garey M. R., Johnson D. S. (1979), *Computers and Intractability: Guide to the theory of NP-Completeness* Freeman; San Francisco
- [36] Gaviro P. S., Ruiz-Lorenzo J. J. and Tarancon A. (2006), J. Phys A **39** 8567
- [37] Geman S. and Geman D. (1984), IEEE Trans. Pattern Anal. Mach. Intell. **6** 721
- [38] Goldschmidt Y. Y. and Lai P.-Y. (1990), Phys. Rev. Lett. **64** 2467
- [39] Grover L. K. (1997), Phys. Rev. Lett. **79** 325
- [40] Guo M., Bhatt R. N. and Huse D. A. (1994), Phys. Rev. Lett. **72** 4137
- [41] Hartmann A. and Rieger H. 2002, *Optimization in Physics*, Wiley VCH, Darmstadt
- [42] Hatano N. and Suzuki M. (2005) in Das and Chakrabarti (2005), pp - 37-67
- [43] Huse D. A. and Fisher D. S. (1986), Phys. Rev. Lett. **57** 2203
- [44] Inoue J.-I. (2005), in Das and Chakrabarti (2005), pp 259-296
- [45] Ishii H. and Yamamoto T. (1985), J. Phys. C **18** 6225
- [46] Jackle J. and Eisinger S. (1991), Z. Phys. B **84** 115
- [47] Kadowaki T. and Nishimori H. (1998), Phys. Rev. E **58** 5355
- [48] Kim D.-H. and Kim J.-J. (2002), Phys. Rev. B **66** 054432
- [49] Kirkpatrick S., Gelatt C.D. and Vecchi M. P. (1983), Science, **220** 671
- [50] Krzakala F., Houdayer J., Marinari E., Martin O. C. and Parisi G. (2001), Phys. Rev. Lett. **87** 197204
- [51] Lancaster D. and Ritort F (1997), J. Phys. A **30**, L41
- [52] Marinari E., Parisi G., Ruiz-Lorenzo J.J. and Zuliani F. (1998) Phys. Rev. Lett. **82** 5176
- [53] Martoňák R., G. E. Santoro and E. Tosatti (2002), Phys. Rev. B **66** 094203
- [54] Martoňák R., Santoro G. E. and Tosatti E. (2004), Phys. Rev. E **70** 057701
- [55] Mezard M., Parisi G. and Virasoro M. A. (1987), *Spin Glass Theory and Beyond* World Scientific Lect. Note in Phys. **9**, Singapore and references therein
- [56] Miller J. and Huse D. A. (1993), Phys. Rev. Lett **70** 3147
- [57] Monasson R., Zecchina R., Kirkpatrick S., Selman B. and Troyansky L. (1999), Nature **400** 133
- [58] Moore M. A., Bokil H. and Drossel B. (1998), Phys. Rev. Lett. **81** 4252
- [59] Morita S. and Nishimori H. (2006), J. Phys. A **39** 13903
- [60] Morita S. and Nishimori H. (2007a), J. Phys. Soc. Jap. **76** 06400
- [61] Morita S. and Nishimori H. (2007b), arXiv:quant-ph/0702252
- [62] Nielsen M. A. and Chuang I. L. (2000) *Quantum Computation and Quantum Information*, Cambridge University Press, Cambridge
- [63] Nishimori H. (2001), *Statistical Physics of Spin Glasses and Information Processing: an Introduction*, Oxford University Press, Oxford
- [64] Papadimitriou C. H. and Steiglitz K. (1998), *Combinatorial Optimization: Algorithm and Complexity*, Dover Publications, New York
- [65] Parisi G. (1980), J. Phys A **13** 1101
- [66] Percus A. and Martin O. C. (1996), Phys. Rev. Lett. **76**, 1188
- [67] Ray P., Chakrabarti B. K. and Chakrabarti A. (1989), Phys. Rev. B **39** 11828
- [68] Rieger H. (2005), in Das and Chakrabarti (2005), pp 69-97
- [69] Roland J. and Cerf N. J. (2001), Phys. Rev. A **65** 042308
- [70] Rodriguez-Laguna J. (2007), J. Stat. Mech. P05008
- [71] S. Sachdev (1999), *Quantum Phase Transitions*, Cambridge Univ. Press, Cambridge
- [72] Santoro G. E., Martoňák R., Tosatti E. and Car R. (2002), Science, **295** 2427
- [73] Santoro G. E. and Tosatti E. (2006), J. Phys. A **39** R393
- [74] Santoro G. E. and Tosatti E. (2007) *News and Views in Nature Physics* **3**, 593
- [75] Sarandy M. S., Wu L.-A., Lidar D. A. (2004) *Quantum Information Processing* **3** 331
- [76] Sarjala M., Petäjä V. and Alva M. (2006), J. Stat. Mech. PO 1008
- [77] Sengupta K., Powell S. and Sachdev S. (2004), Phys. Rev. A **69** 053616
- [78] Sherrington D. and Kirkpatrick S. (1975), Phys. Rev. Lett. **35** 1792
- [79] Schechter M. and Laflorencie N. (2006) Phys. Rev. Lett. **97**, 137204
- [80] Suzuki S. and Okada M. (2005a), J. Phys. Soc. Japan **74** 1649
- [81] Steffen M., Dam v. W., Hogg T., Breyta G., Chuang I. (2003), Phys. Rev. Lett. **90** 067903
- [82] Stella L., Santoro G., and Tosatti E. A. (2005), Phys.

- Rev. B **72** 014303.
- [83] Thirumalai D., Li Q. and Kirkpatrick T. R. (1989), J. Phys. A **22** 2339
- [84] Wu W., Ellman B., Rosenbaum T. F., Aeppli G. and Reich D. H. (1991), Phys. Rev. Lett. **67** 2076
- [85] Wu W., Bitko D., Rosenbaum T. F. and Aeppli G. (1993a), Phys. Rev. Lett. **74** 3041
- [86] Wu W., Bitko D., Rosenbaum T. F., and Aeppli G. (1993b), Phys. Rev. Lett. **71** 1919
- [87] Ye J., Sachdev S. and Read N. (1993) Phys. Rev. Lett. **70** 4011